Inner-shell excitations in weak-bond molecules

I. Ishii, R. McLaren, and A. P. Hitchcock
Department of Chemistry, McMaster University, Hamilton, Ontario L8S 4M1, Canada

M. B. Robin
AT&T Bell Laboratories, Murray Hill, New Jersey 07974

(Received 18 March 1987; accepted 2 July 1987)

It is proposed that Rydberg and valence σ^* conjugate orbitals have separate existences and can be seen in the same spectrum if the σ^* MO can be disentangled from the Rydberg manifold. Because the energy of the σ^* MO is a consequence of the σ–σ^* split resulting from bond formation, the spectra of molecules having weak bonds should show low-lying transitions to σ^* in addition to the conjugate Rydberg bands. Inelastic electron scattering spectra in the x-ray region (270–730 eV) of molecules having bond strengths in the 20–50 kcal/mol regime clearly show well-isolated transitions to low-lying σ^* MOs, and in some cases the simultaneous presence of virtual σ^* and Rydberg conjugate orbitals. The general characteristics of excitations from C 1*s*, O 1*s*, and F 1*s* inner orbitals to σ^* MOs are listed and illustrated by the x-ray spectra of several compounds in which the weak bond involves the O–O or O–F linkage. Quantitative inner-shell optical oscillator strengths derived from the energy loss spectra are reported for H_2O, F_2O, CF_3OF, $CF_3O_2CF_3$, $(CH_3)_3COH$, and $(CH_3)_3CO_2C(CH_3)_3$. The valence-shell spectrum of F_2O also has been determined. Low-lying inner-shell excitations to σ^* valence MOs are identified by their relatively large term values and oscillator strengths. The term values of transitions to σ^* MOs in weak-bond molecules correlate with the relevant bond lengths when considered together with the sum of the atomic numbers of the atoms forming the weak bonds.

I. INTRODUCTION

Our understanding of the electronic spectra of saturated molecules is far less advanced than it is for unsaturated systems containing, for example, pi-electron or *d*-electron chromophores. For saturated systems, a few generalizations can be made which bring the problem into focus:

(1) *All* saturated molecules contain at least one σ bond and except for van der Waals molecules, have at least one occupied σ MO and one vacant antibonding σ^* MO in the ground state. Except for hydrogen, such molecules also will possess lone pair orbitals *n*, which in the most general sense may be taken as either in the outer shell (2*p* on the oxygen atom of water, for example) or in the inner shell (1*s* on the carbon atom of methane, for example).

(2) *All* saturated molecules must exhibit $n \rightarrow \sigma^*$ and/or $\sigma \rightarrow \sigma^*$ excitations in zeroth order.

(3) In addition to the valence excitations terminating at σ^*, *all* neutral molecules will show manifolds of Rydberg transitions below the relevant ionization potentials.

The uninitiated reasonably might expect from the three points listed above that with excitations to σ^* necessarily being a part of every polyatomic molecular spectrum, they would have been studied extensively. There must be a large body of spectral data and interpretation involving σ^* MOs, else how could spectroscopists study the spectra of such key molecules as CH_4, H_2O, C_2H_4, C_6H_6, etc., and feel confident in their interpretation? In reality, almost nothing is known about the excitations to σ^* either in these molecules or in almost all others for that matter, saturated or not. While we are not able to offer a general solution to this pressing problem, we hope to add a new point of view in this work.

For a long time, the spectra of saturated molecules in the region from several eV to several thousand eV were interpreted largely in terms of excitations terminating at σ^* MOs. More recently, the pendulum has swung toward reinterpretation of these spectra as consisting almost totally of Rydberg excitations,[1] leaving the fate of the excitations to σ^* an open question. The answer to this question is further complicated, for Mulliken[2] takes the view that the delineation of excitations as either Rydberg or valence is only a semantic game without any real meaning (for example, he equates the $3sa_1$ Rydberg orbital of methane with the antibonding valence orbital $a_1\sigma^*$), whereas Robin,[1,3,4] Schwarz *et al.*,[5–8] and Lefebvre-Brion and co-workers[9,10] argue for the separate realities of antibonding valence σ^* and Rydberg orbitals, but with allowance for more or less mixing of the two extreme types on a case-by-case basis. In those molecules where the interaction between σ^* and Rydberg MOs is very large, the designation of the resulting MOs as σ^* or Rydberg clearly does lose its meaning. Rydberg–valence orbital pairs such as $3sa_1$ and $a_1\sigma^*$ in methane or $b_2\sigma^*$ and $3pb_2$ in water, which not only belong to the same symmetry representation but also have similar patterns of nodal surfaces are called "Rydberg–valence conjugates."[1] Answers to the three questions concerning (1) the reality of Rydberg–valence conjugates, (2) the reality or uniqueness of excitations to σ^* in saturated molecules, and (3) the energies of excitations to σ^* if they exist, are of prime importance to our understanding of molecular excited states. Of course, the same problems in regard to σ^* MOs exist in π unsaturated and ligand-field molecules as well, but it is possible to avoid them by limiting one's attention to the $\pi \rightarrow \pi^*$ or $d \rightarrow d$ spectra, an option no longer available when dealing with saturated molecules.

There is one class of compounds for which the question of σ^* vs Rydberg conjugate MOs has been answered to ev-

 0021-9606/87/204344-17$02.10

eryone's satisfaction: the alkyl chlorides, bromides, and iodides.[1,4,8,11–13] In these compounds, the lowest excitations to σ^*(C–X) fall well below the lowest Rydberg excitations. An explanation for this unusual situation has been advanced, based upon the energies of the carbon–halogen bonds in the ground state. Referring to Fig. 1, the rationale is as follows. Both the bond strength of the X–Y bond and the splitting between the σ(X–Y) and σ^*(X–Y) MOs depend directly upon the overlap between the X and Y atomic functions given equal or near-equal atomic energies. If the X–Y bond is weak due to a small overlap of the X and Y atomic functions, then there is a small σ–σ^* splitting and thus a low-lying σ^* MO, whereas a strong X–Y bond implies a larger σ–σ^* splitting and thereby a higher energy for $n \rightarrow \sigma^*$ excitation. As expressed in the figure, the lowest σ^* terminating MO may fall below the Rydberg stack if the bond between AX· and ·YB is weak (region I), within it (region II), or above it if the bond is very strong (region III); apparently the alkyl iodides, bromides, and chlorides with their C–X bond energies in the 50–80 kcal/mol range are region I prototypes. The relative positions of σ^* and the Rydberg MOs in the alkyl halides is discussed further in Sec. III C 1.

In this discussion, the phrase "weak-bond" implies the conventional single, two-electron/two-center chemical bond. Note however, that the assumption of a direct relationship between bond energy and σ–σ^* splitting may be too naive in some instances. Thus in cases where there is non-σ bonding ($2p\pi$–$3d\pi$) and/or ionic contributions to the bond, for example, the bond energy may be large whereas the σ–σ^* orbital splitting remains small.

In most saturated molecules, the lowest excitations to σ^* are difficult if not impossible to find, for in most molecules these are in regions II and III. In region II, the σ^* MO falls among the Rydberg levels and frequently is lost due either to spectral congestion or to mixing with and dissolution in the conjugate Rydberg sea. Ammonia and water, with bond strengths in the 110–120 kcal/mol regime are examples of region II chromophores. In region III, the transitions to σ^* usually are very broad due to autoionization and may be easily confused with other processes which also give a cross-section maximum (shake-up, shake-off, two-electron promotion, EXAFS, Cooper minima, etc.). Boron trifluoride is a prime example of a molecule in region III, for its lowest excitations to σ^* fall above the relevant ionization potentials, correlating with its very large B–F bond strength of 153 kcal/mol.

Region I is most inviting if one wishes to study excitation to σ^*, and so one is tempted to focus upon molecules containing a weak bond. This argument is the driving force behind the present study. In particular, we focus upon the spectra of molecules of the sort RO–OR in which there is a weak O–O bond, and RO–F in which there is a weak O–F bond, expecting to find low energy excitations to σ^* MOs in them. Spectra of the corresponding alcohols where available also are determined for comparison with their weak-bond cousins. The bond energies[14] of several relevant species are listed in Table I. Those molecules in Table I which have bond energies in the 20–50 kcal/mol regime are taken as "weak-bond" molecules, with excitations to σ^* most likely to fall below the lowest Rydberg excitation (region I).

The assignment of an observed electronic transition within an independent-particle model requires characterization of both the originating orbital and the terminating orbital. The difficulties in this are reduced considerably by working in a spectral region where the originating orbital is unambiguously determined by the energy of the transition. Thus, for example, excitations at $\sim$300 and at $\sim$540 eV in an alcohol must originate at C 1*s* and O 1*s* inner-shell orbitals, respectively. We thus turn to inner-shell spectra as being inherently easier to interpret; on the other hand, the resolution in these x-ray spectra is far less than for visible/UV spectra. Once the ordering of terminating levels has been determined in the x-ray region, this information then can be applied to spectral interpretation in the visible/UV. It is now well established that spectra obtained by inner-shell electron energy loss spectroscopy (ISEELS)[26] in scattering regimes where electric-dipole transitions dominate are equivalent to optical x-ray absorption spectra. Recent extensions of our ISEELS analysis procedures[27] have been applied in this work to provide an additional dimension to the x-ray spectroscopy in the form of absolute oscillator strengths.

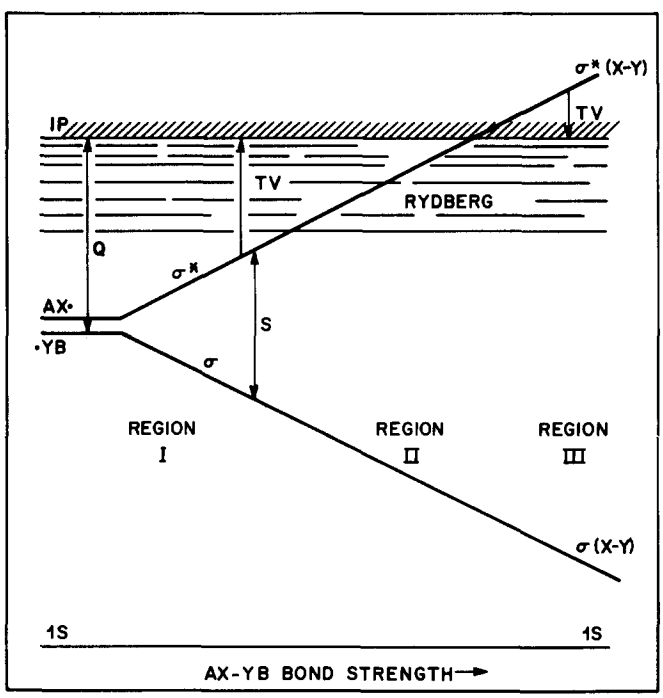

FIG. 1. Relative placement of σ^*(X–Y) and the Rydberg manifold with increasing strength of the X–Y bond. The σ–σ^* splitting S is related to the X–Y bond strength while Q, the average term value of the X· and Y· components prior to X–Y bond formation depends upon the effective nuclear potentials, i.e., the atomic numbers of X and Y. Both S and Q will affect the $1s \rightarrow \sigma^*$(X–Y) term value.

II. EXPERIMENTAL

The C 1*s*, O 1*s*, and F 1*s* inner-shell spectra of F_2O, CF_3OF, CF_3OOCF_3, $(CH_3)_3COOC(CH_3)_3$, and

TABLE I. Selected bond energies, inner shell σ^* term values and distances.

Molecule/bond	Energy, kcal/mol[a]	σ^*TV, eV[b]	Z[c]	R, Å[d]
FKr–F	10.6[e]	10	45	1.875
F_3B–OH_2	~16[f]		13	
F_2N–NF_2	21[g]		14	1.492
$(CO)_5Mn$–$Mn(CO)_5$	22.1[h]			2.977
F–F	36	14.5[i]	18	1.418
$(CH_3)_3CO$–$OC(CH_3)_3$	37	8.8	16	1.480[j]
FO–F	38.4[k]	11.3(11.8)	17	1.405
CF_3O–F	43.5[l]	11.1	17	1.421
F_3CO–OCF_3	46.2[g]	8.3	16	1.419[j]
HO–OH	51		16	1.475
H_3Si–SiH_3	51	...[m]	28	
H_2N–NH_2	60	1.6	14	1.45
H–I	70	6.8	54	1.61
H_3C–CH_3	80	−0.5	12	1.533
$(CH_3)_3Sn$–$Sn(CH_3)_3$	80[g]			
H–Br	86	6.7	36	1.41
HOO–H	90		9	0.950
H_2N–H	102		8	1.012
H–Cl	102	6.4	18	1.27
O–O	118	−1.9[i]	16	1.207
HO–H	118		9	0.958
H–F	134	6.7	10	0.92
F_2B–F	153[n]	−2.3[n]	14	1.307
N–N	225	−9.0	14	1.095

[a] Bond energies from Ref. 14 unless otherwise noted.
[b] Term values from this work (and unpublished), unless otherwise noted. Theoretical inner-shell σ^* term values as predicted by the empirical TV–R relationship (Ref. 15) are given in parentheses.
[c] Z is the sum of the atomic numbers of the atoms forming the bond indicated in the molecular formula.
[d] Bond lengths from Ref. 16 unless otherwise indicated.
[e] Reference 17.
[f] Reference 18.
[g] Reference 19.
[h] Reference 20.
[i] Reference 21.
[j] Reference 22.
[k] Reference 23.
[l] Reference 24.
[m] Value unknown for Si_2H_6, but is approximately 4 eV for $Si_2(CH_3)_6$.
[n] Reference 25.

$(CH_3)_3COH$ were recorded by electron energy loss spectroscopy with the McMaster ISEEL spectrometer operated under dipole-dominated conditions (2.5 keV final electron energy and scattering angles less than 2°).

The resolution of 0.6 eV FWHM is dictated largely by the energy width of the unmonochromatized incident electron beam. Further details on the ISEEL spectrometer and operating procedures have been presented elsewhere.[21,28] Each of the samples is a commercial product (F_2O, Ozark Mahoning; CF_3OF and CF_3OOCF_3, SCM Corp.; $(CH_3)_3COOC(CH_3)_3$, Pfaltz and Bauer; $(CH_3)_3COH$, Fischer Scientific). The purities of the samples were monitored inside the ISEEL spectrometer using a quadrupole mass spectrometer. Liquid samples were subjected to several freeze–pump–thaw cycles in order to remove dissolved air and any other volatile impurities. In all cases except F_2O, the energy loss spectra were determined with a sample pressure of $\sim 10^{-4}$ Torr in the collision cell. For F_2O, a reduced pressure of $\sim 10^{-5}$ Torr was used in order to minimize damage to the spectrometer from this highly reactive material. (Note that extreme caution is necessary when handling CF_3OF and F_2O because of the violent reactions that can occur between them and other organic materials.) Calibration of the inner-shell spectra was effected by the addition of CO, CO_2, O_2, or N_2 as appropriate. In the O 1s spectra of the two peroxides, weak bands observed at 532 eV are attributed to O_2 as an impurity, while the C 1s and O 1s spectra of CF_3OF contain contributions from CO_2 as an impurity. Energy losses arising from the impurities have been removed from the spectra by subtraction of appropriately scaled spectra of O_2 and CO_2, recorded under identical conditions. The procedure employed in converting the recorded energy-loss amplitudes into absolute optical oscillator strengths is presented in Sec. III D.

III. RESULTS AND DISCUSSION

A. Predictions for inner-shell excitations in weak-bond molecules

For purposes of interpretation, we consider not only the energy of the excitation with respect to the ground state of the neutral molecule, but also with respect to that of the ion formed by removal of an electron from the originating MO. This latter energy difference is called the term value (TV in Fig. 1) and takes on characteristic values depending upon the nature of the terminating orbital.[1] Not only is the term value of great use in distinguishing between (1s, σ^*) valence and (1s, R) Rydberg excited states, but in the former it also correlates well with specific bond distances and so has a possible use in determining spectral assignments and/or molecular structure.[15,21,29] This well-documented relationship between (1s, σ^*) term value and bond length is used here to guide our spectral assignments since the molecular structures are known.[16,22]

We list several general expectations regarding excitations to σ^* MOs in inner-shell spectra.

(i) Whereas the term values of the lowest-lying inner-shell Rydberg excitations do not exceed 6 eV, and often are far smaller, those of $n \rightarrow \sigma^*$ excitations in weak-bond molecules (region I) can be far larger (Table I). The (n, σ^*) term values in molecules having bond strengths appropriate to regions II and III will equal approximately those of the conjugate Rydberg excitations or will be negative, respectively (Fig. 1).

(ii) Molecules containing both weak bonds and strong bonds will show transitions to σ^* MOs in both regions I and II/III.

(iii) The term values of $n \rightarrow \sigma^*$(X–Y) transitions where the X–Y bond is weak will be similar in the X 1s and Y 1s spectra even though these spectral regions might be hundreds of eV apart.

(iv) Energies of the (n, R) Rydberg levels will be unaffected by where the σ^* MOs fall, except possibly for the lowest Rydberg levels of s and p type. In this case, the 3s and certain 3p orbitals may interact strongly with their conjugate σ^* MOs due to their large penetration. If the spectral type is that of region I, then the conjugate mixing with σ^* can act to make the (n, 3s) and (n, 3p) Rydberg term values abnor-

mally small, whereas a region II situation leads to abnormally large $(n, 3s)$ and $(n, 3p)$ Rydberg term values. Mixing of these Rydberg excited states with their σ^* valence conjugates will intensify the former at the expense of the latter.

(v) A low-lying excitation to σ^* in the outer-shell spectrum of a molecule implies related low-lying excitations in the inner-shell spectra originating at the atoms involved in the σ^* orbital.

(vi) In accord with the expected inverse relationships between bond length and bond strength, and that between bond strength and term value [point (i) above], the (n, σ^*) term value will depend directly upon the appropriate σ bond length,[15,21] with due consideration also being given to the sum of atomic numbers of the relevant atoms (*vide infra*).

(vii) Inner-shell excitations to low-lying σ^* MOs which are electric-dipole allowed will be relatively very intense, for the spatial overlap of $1s$ with valence σ^* MOs will be larger than with Rydberg orbitals. For compounds in region II, the $n \rightarrow \sigma^*$ intensity will not be as prominent, for the (n, σ^*) configuration will be mixed more or less into the surrounding Rydberg levels. Excitations to σ^* in region III molecules generally will be very broad, although exceptions to this generality are known.

(viii) $n \rightarrow \sigma^*$ intensity develops in the inner-shell spectra of only those atoms on which σ^* has significant density. If the low-lying σ^* MO is the result of a weak bond between atoms X and Y, then the transitions to σ^* will be most intense relatively in the X $1s$ and Y $1s$ spectra, and absent when originating at other atoms, which will show Rydberg transitions and transitions to σ^* in regions II and/or III.

(ix) The relative intensities of X $1s \rightarrow \sigma^*$(X–Y) and Y $1s \rightarrow \sigma^*$(X–Y) transitions will reflect both the relative atomic $\langle 1s|\mathbf{er}|2p\rangle$ transition moments (squared) and the relative weights of the X and Y atomic orbitals in the σ^* wave function. Assuming a localized core hole in a molecule composed of first-row atoms (H through F), the squared transition moment $|\langle 1s|\mathbf{er}|\sigma^*\rangle|^2$ governing the X $1s \rightarrow \sigma^*$ oscillator strength will be proportional to four factors: (1) the number of X atoms involved in the weak σ^* MO, (2) the square of the coefficient of the X atom AO in σ^*, (3) the fraction of $2p$ character in the X-atom AO involved in σ^*, and (4) the square of the inherent atomic transition moment $|\langle \text{X } 1s|\mathbf{er}|2p\rangle|^2$. (The oscillator strength also depends directly upon the transition energy.) Inasmuch as factors (2) and (3) are necessarily equal to or less than unity, the atomic X $1s \rightarrow 2p$ oscillator strength is an approximate upper limit to the valence X $1s \rightarrow \sigma^*$ oscillator strength on a per-X-atom basis.

(x) Excitations to σ^* generally will be broader than those to Rydberg orbitals because the Rydberg orbitals are nonbonding whereas the σ^* MOs are antibonding. The $(1s, \sigma^*)$ states will be strongly dissociative.

(xi) Configurations based on inner-shell excitations to σ^* and to Rydberg orbitals will give rise to both singlet and triplet states. As with the oscillator strengths, the singlet–triplet splittings will depend upon $1s/\sigma^*$ or $1s$/Rydberg orbital overlap, and so will be far larger for transitions terminating at σ^* valence MOs than for those terminating at Rydberg MOs. Observation of the singlet→triplet excitations using ISEELS is facilitated by using large angle scattering at near-threshold impact energies. Under these conditions, $^3\Pi$–$^1\Pi$ splittings up to 1.5 eV have been observed recently in inner-shell spectra.[30] Splittings of similar magnitude are expected for intense $1s \rightarrow \sigma^*$(X–Y) transitions.

(xii) In a weak-bond molecule AX–YB, excitations from A to σ^*(X–Y) may have a very weak but detectable intensity. Because the transition involves a significant charge transfer (A→X–Y), its term value will be smaller than for the corresponding transitions originating at X or Y.

Let us now take these qualitative ideas as guides to the interpretation of the x-ray spectra of weak-bond molecules. The spectral aspects of interest to us are transition energies, term values, and oscillator strengths in the regions of the inner-shell ionization potentials. Many of the expected spectral features listed above are realized in the x-ray spectra of the weak-bond molecules F_2O, CF_3OF, CF_3OOCF_3, and $(CH_3)_3COOC(CH_3)_3$; these are discussed in the context of the spectra of related "strong-bond" molecules in the subsequent sections.

B. Weak-bond spectra

1. Oxygen difluoride

As expected for a saturated molecule with strong bonds, the O $1s$ electronic excitations of water (Fig. 2) are primarily of Rydberg character (as are the outer-shell transitions[1]), albeit with somewhat large term values and intensities for the excitations terminating at $3s$ and $3pb_2$, Table II. The O $1s$ spectrum of H_2O newly recorded for this work is in excellent agreement with that reported by Wight and Brion.[31] In the case of F_2O, it is calculated that the overlap population in the O–F bond is much smaller than that in the O–H bond of H_2O,[33] and indeed, the bond energies for F_2O and H_2O are reported to be 38.4[23] and 119 kcal/mol,[14] respectively. This very large disparity in bond energies leads one to expect very large differences in the electronic spectra of F_2O and H_2O in regard to σ^* MOs, as is the case. The Rydberg features in both the O $1s$ and F $1s$ spectra of F_2O (Fig. 3 and Table II) appear to be regular, with term values roughly similar to those in H_2O and with the intensity to $3p$ larger than that to $3s$. However, these Rydberg excitations in F_2O are dwarfed by the broad, intense features at 534.6 and 683.75 eV, bands for which there are no counterparts in H_2O, Fig. 2. It is clear from the term values of these bands of F_2O (approximately 11 eV in both the O $1s$ and F $1s$ spectra) that they must terminate at σ^*(O–F). Note that the O $1s \rightarrow \sigma^*$ transition in F_2O is more than ten times as intense as the entire Rydberg spectrum integrated up to the ionization limit. As measured by term values and intensities, it is clear that the O–F bond of F_2O is a region I chromophore, whereas the O–H bond of H_2O is region II.

According to the theoretical work of Valenta *et al.*,[34] the lowest σ^* MO in F_2O has a_1 symmetry and so O $1s \rightarrow \sigma^*$ is an allowed excitation. Most interestingly, the excitation from O $1s$ to the second σ^* orbital (b_2) also is allowed formally, yet no second *intense* transition is apparent. One possibility for a second transition to σ^* from O $1s$ in F_2O is the band at 549.6

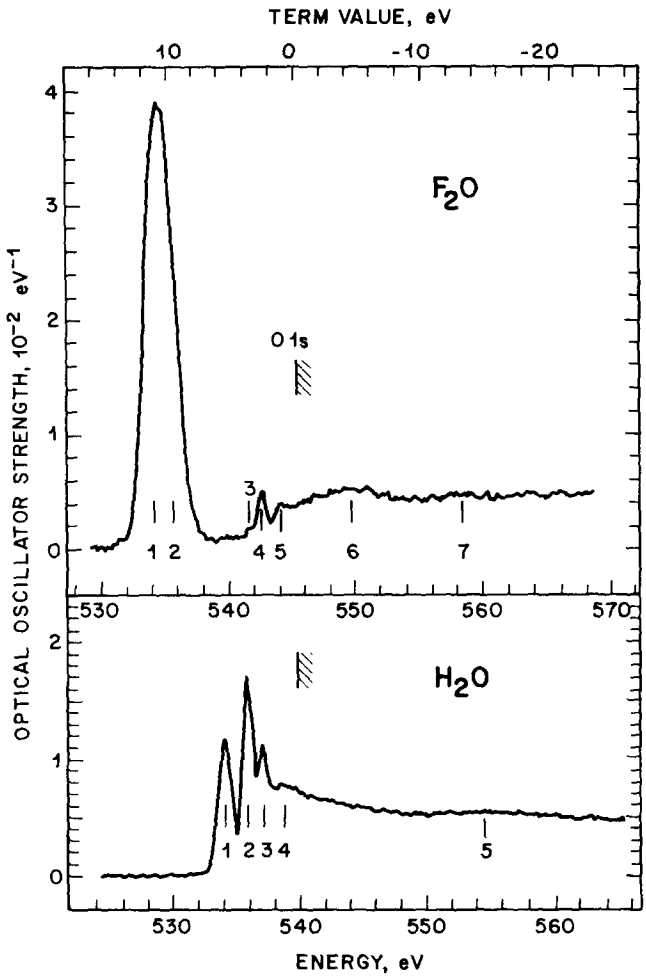

FIG. 2. Quantitative comparison of the O 1*s* optical oscillator strength spectra of F_2O and H_2O, shifted so as to align the O 1*s* ionization potentials. The final electron energy is 2.5 keV, the scattering angle is 2°, and the resolution is 0.6 eV FWHM. The spectra shown are the result of the conversion of the raw data to absolute optical oscillator strength scales as described in the text.

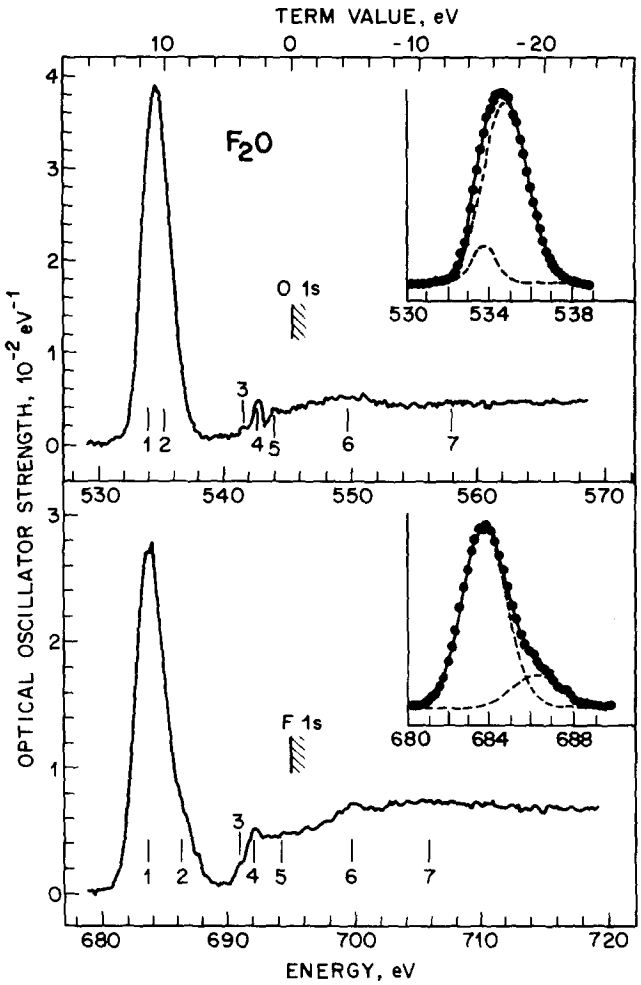

FIG. 3. Inner-shell energy loss spectra of oxygen difluoride, expressed in optical oscillator strength in the region of the O 1*s* (upper) and F 1*s* ionization potentials (lower). The inset figures show resolutions of the lowest bands into sums of two Gaussians as determined by least-squares fitting.

TABLE II. Inner-shell excitations (ΔE, eV), term values (TV, eV), and oscillator strengths (f, 10^{-2}) in H_2O and F_2O.

H_2O (O 1*s*)				F_2O (O 1*s*)				F_2O (F 1*s*)				
Band	ΔE	TV	f	Band	ΔE	TV	f	Band	ΔE	TV	f	Assignment
	...	...		1[a,c]	533.7	11.6	1.0	1[b,c]	683.75	11.3	7.4	$5a_1\sigma^*$(O–F)
	...	...		2[a,c]	534.8	10.5	9.6	2[b,c]	686.24	8.8	1.4	$4b_2\sigma^*$(O–F)
1	534.0	5.7	1.4	3	541.6	3.7	0.07	3	691.0	4.0	0.15	$3s/\sigma^*$ [d]
2	535.9	3.8	1.6		...	...			...	...		$3pb_2/\sigma^*$ [d]
3	537.1	2.6	1.2	4	542.6	2.7	0.41	4	692.2	2.8	0.66	$3p/\sigma^*$ [d]
4	538.5	1.2	0.9	5	544.0	1.3	0.56	5	694.2	0.8	0.9	$4p'/\sigma^*$ [d]
	539.7[e]	0	...		545.33[f]	0			695.07[f]	0		IP
	...	...		6	549.6	−4.3		6	699.8	−4.8		2*e*?
5	555	−15		7	558(?)	−13		7	706	−11		Shake-up?

[a] Maximum calibrated as 534.6 eV, 3.82 eV above the $1s\rightarrow\pi^*$ transition of O_2 at 530.8 eV.

[b] Maximum calibrated as 683.8 eV, 149.2 eV above the O $1s\rightarrow\sigma^*$ transition of F_2O at 534.6 eV.

[c] A least-squares fit to a sum of two Gaussians results in these energies and oscillator strengths (see inserts to Fig. 3) with χ^2 values of 0.08 (O 1*s*) and 0.04 (F 1*s*). However, four fits to the O $1s\rightarrow\sigma^*$(O–F) profile were readily obtained which were visually as good as that quoted in the table. These fits, with χ^2 values between 0.12 and 0.21, gave average peak energies of 534.1 and 535.3 eV, and average oscillator strengths ($\times 10^{-2}$) of 4.5 and 6.1, respectively.

[d] Some σ^*(O–H) character is likely for these features of H_2O. By contrast, the corresponding transitions in F_2O are more purely Rydberg in character.

[e] Reference 31.

[f] Reference 32.

eV (band 6), which has a counterpart at 699.8 eV in the F 1*s* spectrum. However this assignment results in an $a_1\sigma^*$–$b_2\sigma^*$ split of 15 eV, which seems extreme in view of the facts that the separation of the corresponding occupied $3a_1\sigma$–$3b_2\sigma$ ground-state MOs is only ~3 eV[35] and that Von Niessen[36] calculates the $5a_1\sigma^*$–$4b_2\sigma^*$ virtual-orbital splitting in F_2O to be only 1.07 eV. Were the $a_1\sigma^*$–$b_2\sigma^*$ splitting in F_2O as small as 1 eV, then the two allowed $1s\rightarrow\sigma^*$ transitions in both the O 1*s* and F 1*s* spectra would be barely resolved. Indeed, as shown in the insets of Fig. 3, the F $1s\rightarrow\sigma^*$(O–F) profile has a distinct high-energy shoulder and the full profile is unambiguously fitted by two Gaussian components separated by 2.2 eV. The best fit to the O $1s\rightarrow\sigma^*$(O–F) profile indicates a separation of 1.1 eV, with inversion of the relative intensities as compared with the F $1s\rightarrow\sigma^*$(O–F) transition. However, this fit is not unique, since others were found which were visually satisfactory, although with χ^2 values 1.5 to 2.5 times larger. In spite of the ambiguity, in every case the $5a_1\sigma^*$–$4b_2\sigma^*$ splitting in the O 1*s* spectral decomposition was 1–2 eV. We conclude that each of the lowest peaks in Fig. 3 actually consists of two allowed transitions: $1s\rightarrow5a_1\sigma^*$(O–F) and $1s\rightarrow4b_2\sigma^*$(O–F). The relative intensities of the transitions to $5a_1$ and $4b_2$ in the O 1*s* and F 1*s* spectra indicate that the $5a_1$ σ^* orbital has a much greater density on the fluorine atoms, whereas $4b_2$ σ^* is oxygen localized. It follows from our assignment of the $5a_1\sigma^*$–$4b_2\sigma^*$ splitting as 1–2 eV that the broad transitions at 549.6 and 699.8 eV in F_2O cannot be one-electron excitations terminating at σ^*; they are tentatively assigned as two-electron excitations.

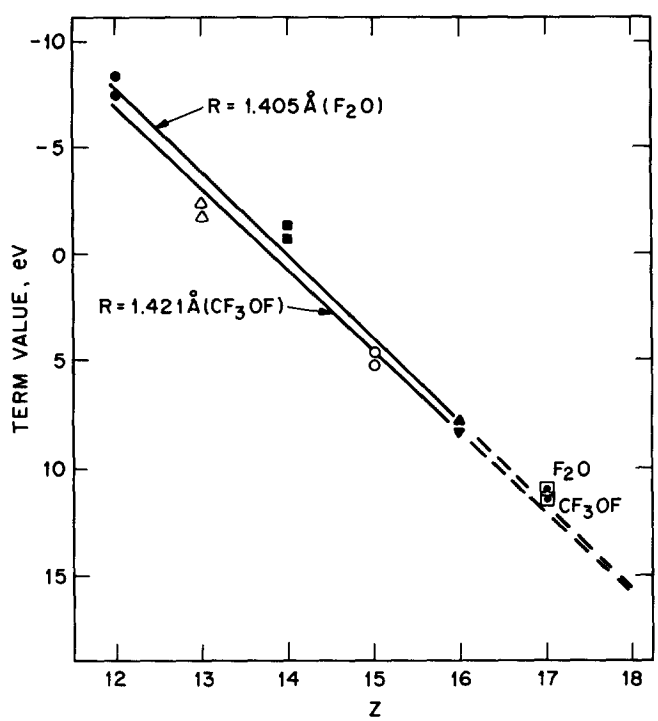

FIG. 4. Plot of the (1*s*, σ^*) term value vs *Z*, the sum of atomic numbers of the two atoms involved in the σ bond. The points between $Z = 12$ and 16 are calculated for bond lengths of 1.405 Å (F_2O) and 1.421 Å (CF_3OF), while the points at $Z = 17$ are those found for F_2O and CF_3OF in this work.

The energies of the transitions to σ^* in both the F 1*s* and O 1*s* spectra are consistent with the previously documented correlation between (1*s*, σ^*) term values and bond lengths.[15,21] In Refs. 15 and 21, a parameter $\delta = \Delta E - \mathrm{IP} = -\mathrm{TV}$ was used, rather than the term value. According to the correlation, the term value depends on both *R* (the bond length, 1.405 Å for F_2O[16]) and *Z* (the sum of the atomic numbers of the atoms forming the bond, 17 for F_2O). Because F_2O represents one of only two members of the $Z = 17$ correlation line, we demonstrate its consistency with past results by first calculating the term value at $R = 1.405$ Å for *Z* between 12 and 16. The extrapolation of this line to $Z = 17$, $R = 1.405$ Å predicts a (1*s*, σ^*) term value of 11.8 eV for F_2O (Fig. 4). This is in good agreement with the term values [10.7 (O 1*s*) and 11.3 eV (F 1*s*)] observed for the lowest resolved $1s\rightarrow\sigma^*$(O–F) excitations in the O 1*s* and F 1*s* spectra.

As can be seen in Table III, the σ^*(O–F) term value determined for F_2O fits nicely into the series observed for first row fluorides from BF_3 to F_2. This series shows in a striking way how the σ^* term value varies inversely with the corresponding bond energy and linearly with *Z*. It is noteworthy that these term values have a better linear fit to *Z* (correlation coefficient $r = 0.998$) than to bond energy (correlation coefficient $r = 0.973$); the bond length varies systematically in this series from 1.31 Å in BF_3 to 1.42 Å in F_2.

The comparison of Rydberg inner-shell term values in H_2O and F_2O (Table II) is worthy of comment in light of point (iv) above. The observation of anomalously large inner-shell and outer-shell term values for transitions terminating at $3sa_1$ and $3pb_2$ Rydberg orbitals in H_2O implies that the as-yet unidentified conjugate $a_1\sigma^*$ and $b_2\sigma^*$ valence MOs lie above the Rydberg orbitals, so that the mixing of these conjugates depresses the latter. By contrast, in F_2O the corresponding zero-order σ^* MOs are considerably *below* their conjugate Rydberg levels. As a result, the (1*s*, 3*s*) term values are normal while the $3pb_2$ MO is unresolved from the other 3*p* components, again as is normally the case.[1] Note that the F_2O inner-shell spectra show not only the two possible excitations to the σ^* valence MOs, but also that to the conjugate 3*s* Rydberg MO as well (and possibly that to $3pb_2$). The simultaneous presence of conjugate Rydberg and valence transitions in a molecular spectrum is a rare event,

TABLE III. Bond energies and (1*s*, σ^*) term values in the first-row fluorides.

Molecule	*Z*[a]	Bond energy, kcal/mol[b]	(1*s*, σ^*) term value,[c] eV	Region
BF_3	14	153	−2.3	III
CF_4	15	116	3.3	II
NF_3	16	65	6.6	I
OF_2	17	38.4	11.3	I
FF	18	36	14.5	I

[a] Sum of atomic numbers of the two bonded atoms.
[b] See Table I for references.
[c] From Ref. 15, which contains references to the original literature.

and supports the argument for the separate existence of these conjugate electronic configurations in at least some if not all molecules.[1,3–10]

As a consequence of the decreased mixing of Rydberg and conjugate configurations in F_2O, the oscillator strength for the Rydberg region in the O 1*s* spectrum of F_2O (538–545 eV) is considerably smaller than that for the corresponding region of H_2O where mixing with σ^* intensifies the transitions to 3*s* and $3pb_2$, Fig. 2. As seen in the figure and Table II, the excitation to σ^*(O–F) in F_2O is more intense than any single excitation in H_2O, and results in a ratio of discrete to continuum intensity of 1.45 in the former compared to only 0.37 in the latter, Table IV. Alternatively, the lower intensities of the Rydberg spectrum of F_2O may be viewed as a consequence of the potential barrier generated by the F atoms.[37] This barrier acts to distance the Rydberg electron from the molecular core, transforming the wave function into an "outer-well" level. This not only lowers the $1s \rightarrow R$ transition densities as compared to the situation in H_2O, but also lowers the Rydberg term values, as observed. With regard to valence excitations, the barrier generated by the F atoms also acts to form a localized inner-well level (σ^*) having a large electric-dipole moment matrix element with 1*s*. The descriptions of these upper levels in terms of valence and Rydberg MOs on the one hand, and in terms of inner-well and outer-well levels separated by a potential barrier on the other, are thought to be equivalent.

The inner-shell spectral results can be applied to the outer-shell spectrum of F_2O. The lowest ionization potential of F_2O is 13.25 eV[35]; given this and an inner-shell (n, σ^*) term value of 11.3 eV which must be diminished by ~0.7 eV to account for the higher effective nuclear charge in an inner-shell excited configuration (so-called "exhaltation" [1]), leads to the expectation of an excitation to σ^* at ~3 eV in the visible spectrum. Indeed, F_2O is described as a pale yellow gas[34] in strong contrast to the colorless nature of H_2O. In order to place this observation on a more quantitative footing, we have determined the F_2O outer-shell spectrum by electron impact at 2.5 keV final energy and 2° scattering angle, Fig. 5. A weak energy loss at 4.64 eV with a term value of 8.6 eV is observed. This likely is the $2b_2 \rightarrow a_1\sigma^*$ transition predicted by Valenta *et al.* to come at 5.6 eV; its low energy is a direct consequence of the low strength of the O–F bond. Figure 5 represents the first report of the valence-shell excitation spectrum of F_2O to our knowledge. The photoionization efficiency curves for producing F_2O^+ and OF^+ from F_2O have been presented by Berkowitz *et al.*[38] The positions of the photoionization peaks observed by Berkowitz *et al.* in the 14–19 eV region are in reasonable agreement with structures in Fig. 5, although relative intensities differ and not all of the energy-loss features above the first ionization potential (13.1 eV) appear in the photoionization curves.

TABLE IV. Integrated oscillator strengths ($\times 10^{-2}$)[a] below and above the inner-shell ionization potentials.

Compound (orbital)	IP, eV	Σf (discrete)[b] Total	Σf (discrete)[b] Per atom	f' (continuum)[c] Total	f' (continuum)[c] Per atom	$\Sigma f/f'$
(C 1*s*)						
$(CH_3)_3COH$	290.5	21.4	5.9	113	28.1	0.19
$[(CH_3)_3CO]_2$	290.5[d]	45.3	5.7	231	28.9	0.19
$CF_3O_2CF_3$	300.8	78.6	39.3	45.0	22.5	1.75
CF_3OF	301.1	45	45	23.5	23.5	1.91
(O 1*s*)						
H_2O	538.9	5.2	5.2	13.7	13.7	0.38
$(CH_3)_3COH$	538.4	5.5	5.5	15.7	15.7	0.35
$[(CH_3)_3CO]_2$	541.5[d]	26.5	13.3	31.6	15.8	0.84
$CF_3O_2CF_3$	541.9	21.8	10.9	34.3	17.1	0.64
CF_3OF	543.6	18.1	18.1	16.5	16.5	1.10
F_2O	545.3	18.8	18.8	13[e]	13	1.45
(F 1*s*)						
$CF_3O_2CF_3$	694.7	31.1	5.2	72.8	12.1	0.43
CF_3OF	695.0	23.4	5.9	44.8	11.2	0.52
F_2O	695.1	12.3	6.1	19	9.5	0.65

[a] One unit of oscillator strength corresponds to 109.7 Mb in cross section.
[b] The sum of all oscillator strengths of bands below the stated ionization potential.
[c] The integrated oscillator strength from the ionization potential to 25 eV higher energy.
[d] Estimated values.
[e] Obtained by extrapolating the measured curve by 3 eV so as to reach 25 eV beyond the ionization potential.

2. Trifluoromethyl hypofluorite

As with F_2O, trifluoromethyl hypofluorite (CF_3OF) has a small O–F overlap population[39] and an O–F bond energy of only 43.5 kcal/mol[24]; thus one again expects a low-lying σ^*(O–F) MO. The outer-shell spectrum of CF_3OF shows this to be the case, with the lowest energy electronic transition being extremely nonvertical and having a term value of over 7 eV,[40] whereas the lowest observed Rydberg excitation has a term value of only 2.5 eV. It is no surprise then, Fig. 6 and Table V, that the lowest-energy excitations in the O 1*s* and F 1*s* inner-shell spectra of CF_3OF exhibit term values (11.0 and 11.1 eV) which are far too large to support Rydberg assignments. (The 1*s* ionization potentials used for the calculation of the CF_3OF term values, Table V, were deduced from those tabulated for related compounds[41]; the near equality of the term values of the lowest energy

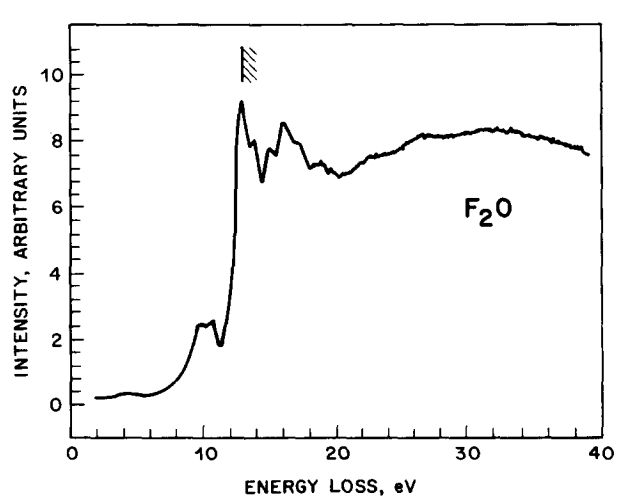

FIG. 5. Outer-shell energy loss spectrum of oxygen difluoride taken at a final electron energy of 2.5 keV and 2° scattering angle. The left-hand edge of the hatched area indicates the first ionization potential.

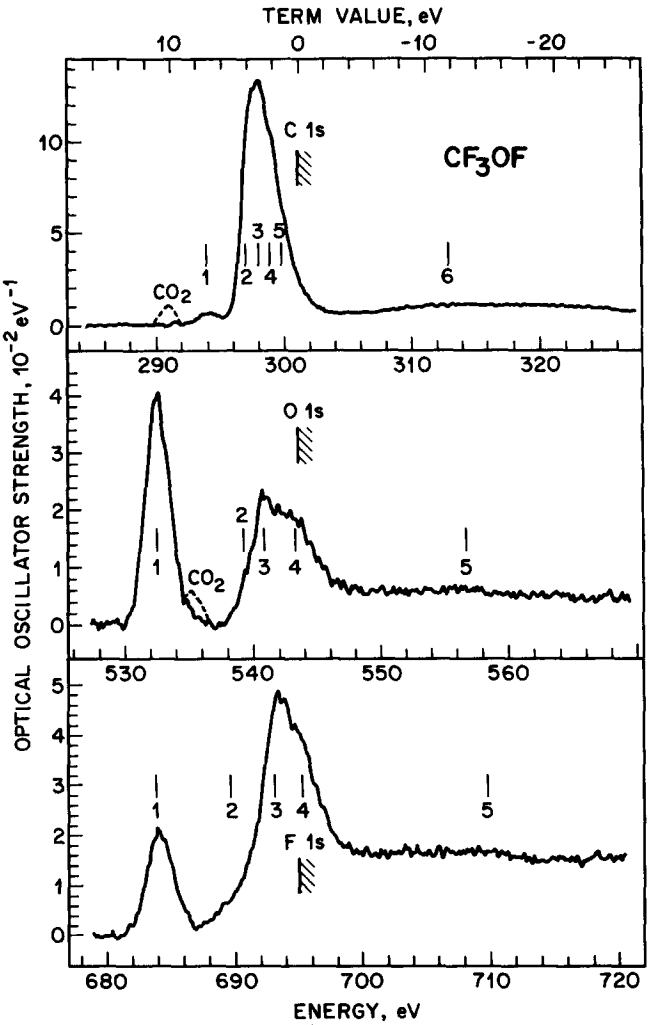

FIG. 6. Optical oscillator strengths derived from the inner-shell energy loss spectra of trifluoromethyl hypofluorite recorded with a final electron energy of 2.5 keV, a 2° scattering angle, and a resolution of 0.6 eV FWHM. Estimated ionization potentials are indicated by the left-hand edges of the hatched areas. The signal due to a small amount of CO_2 impurity has been subtracted from the raw data to produce the C 1*s* and O 1*s* spectra shown as full curves. The dashed curves labeled "CO_2" indicate the contributions of the most intense $1s\rightarrow\pi^*$ transitions of CO_2 to the as-recorded spectra.

excitations in the O 1*s* and F 1*s* spectra suggests that the estimated ionization potentials are close to the true ones.) The term values in CF_3OF closely match those of the lowest energy bands in F_2O (O 1*s*, 10.7 eV; F 1*s*, 11.3 eV) where the transitions are assigned as terminating at σ^*(O–F). It is clear as well from the relative weakness of the excitation to σ^*(O–F) in the C 1*s* spectrum (band 1) compared to its intensities in the O 1*s* and F 1*s* spectra of CF_3OF that the excitation terminates at σ^*(O–F). The near-equality of the [1*s*, σ^*(O–F)] term values in F_2O and CF_3OF implies a near equality of (O–F) bond lengths, Fig. 4, and this is observed (1.405 vs 1.421 Å). The remaining features in the spectra of CF_3OF are assigned as in Table V. In this, we note that several term values are compatible both with Rydberg assignments and with assignments to region II/III σ^* valence MOs as deduced from bond lengths. These are described simply as R/σ^*, without implying the relative importance of the two components, although the strong intensity in the discrete region (Table IV) is suggestive of a large valence contribution.

3. Alkyl peroxides

According to Table I, the two peroxides di(*t*-butyl) peroxide [$(CH_3)_3CO$–$OC(CH_3)_3$] and bis-trifluoromethyl peroxide (CF_3O–OCF_3) have weak O–O bonds,[42,43] with energies approximately equal to that of the O–F bonds of F_2O and CF_3OF. The inner-shell spectra of these peroxides (Figs. 7 and 8, and interpreted in Tables VI and VII) show the low-lying excitations to σ^*(O–O) MOs expected of region I chromophores. As in the cases of F_2O and CF_3OF, the O $1s\rightarrow\sigma^*$ energy loss at 533.6 eV (band 1) in $CF_3O_2CF_3$ dominates the spectrum (Fig. 7), and has a term value (8.3 eV) which is far too large to permit a Rydberg assignment. That the transition to σ^* is so prominent in the O 1*s* spectrum of $CF_3O_2CF_3$ whereas it is very weak or absent in the C 1*s* and F 1*s* spectra illustrates point (viii) above. That is to say, the intensities to σ^* are largest when originating at atoms where σ^* has the largest density. The spectra in Fig. 7 show in a dramatic way that the σ^* MO in question is strong-

TABLE V. Inner-shell excitations (ΔE, eV), term values (TV, eV), and oscillator strengths (f, 10^{-2}) in CF_3OF.

C 1*s*				O 1*s*				F 1*s*				
Band	ΔE	TV	f	Band	ΔE	TV	f	Band	ΔE	TV	f	Assignment
1	294.1	7.0	1.1	1	532.5[a]	11.1	6.7	1	684.0[b]	11.0	5.2	σ^*(O–F)
2	297.4	3.7		2	539.3	4.3		2	690	5.0		3*s*
3	298.0[c]	3.1	43.3	3	540.8	2.8	6.7	3	693.5	1.3	26	3*p*/σ^*(C–F)
4	298.8	2.3										3*p*′
5	300	1.1		4	543	0.5		4	695	0.0		R/σ^*(C–O)
	301.1[d]				543.6[d]				695.0[d]			IP
6	313	−12		5	557	−13		5	710	−14		EXAFS?

[a] Calibrated as 2.90 eV below the O $1s\rightarrow\pi^*$ transition of CO_2 (535.4 eV).
[b] Calibrated as 149.8 eV above the O $1s\rightarrow\pi^*$ transition of CO (534.2 eV).
[c] Calibrated as 10.6 eV above the C $1s\rightarrow\pi^*$ transition of CO (287.40 eV).
[d] Estimated ionization potentials deduced in the following way: C 1*s* equal to that in CF_3OCF_3; O 1*s* average of those in CF_3OCF_3 (541.9 eV) and F_2O (545.3 eV); F 1*s* average of those in CF_3OCF_3 (694.9 eV) and F_2O (695.1 eV) (Ref. 41).

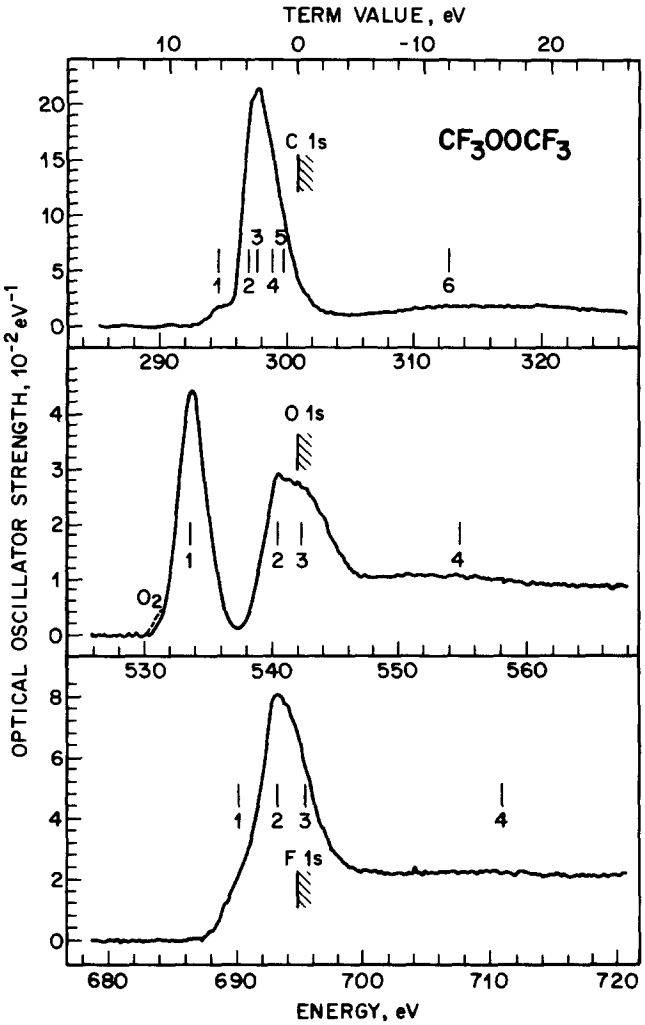

FIG. 7. Optical oscillator strengths derived from the inner-shell energy loss spectra of bis-trifluoromethyl peroxide recorded in the regions of the C 1*s* (upper), O 1*s* (middle), and F 1*s* ionization potentials (lower). The final electron energy is 2.5 keV, the scattering angle is 2°, and the resolution is 0.6 eV FWHM. The signal due to a small amount of O_2 (O $1s \rightarrow \pi^*$, dashed line in the O 1*s* spectrum) has been subtracted from the raw data to produce the full curve shown here.

ly oxygen localized and so justifies experimentally our description of this MO as σ^*(O–O) in CF_3OOCF_3. The large differences in the intensities of transitions to σ^*(O–O) from the various atomic 1*s* orbitals of $CF_3O_2CF_3$ clearly demonstrate the utility of inner-shell spectroscopy in mapping the spatial distribution of virtual valence orbitals. This aspect of ISEELS has been employed recently to determine quantitatively the distribution of the π^* molecular orbital among the C, O, and X atomic orbitals of substituted carbonyls (HCOX with X = NH_2, OH, and F),[45] and similar analyses have been made for the fluoroethylenes.[27]

The C 1*s* spectrum of $CF_3O_2CF_3$ is dominated by a poorly resolved cluster of transitions centered at ~298 eV (bands 2–5). Features with similar term values, widths, and equally prominent intensities are observed in the C 1*s* spectra of molecules containing the CF_3 group, as for example, in CF_3OF (Fig. 6), perfluoroethane and perfluoroneopentane.[46] These bands have been assigned as terminating at orbitals which are hybrids of 3*s* and 3*p* Rydberg MOs, strongly mixed with their σ^* (C–F) conjugate valence MOs. The F 1*s* spectrum of $CF_3O_2CF_3$ is dominated by a broad band around 694 eV having shoulders on both sides. This feature is similar to the second band in the F 1*s* spectrum of CF_3OF (Fig. 6), indicating that we are dealing with an excitation which is characteristic of the CF_3 group. These broad F 1*s* features are similar to those observed in saturated perfluorocarbons such as C_2F_6 and $C(CF_3)_4$.[46] In these, the upper orbitals are assigned as mixed Rydberg/valence shell, with large σ^*(C–F) character. The term values of the F $1s \rightarrow R/\sigma^*$(C–F) transitions are systematically 1.5–2.5 eV smaller than those for the corresponding features in the C 1*s* spectra of the fluorocarbons.[27,46,47] The high energy shoulders in the F 1*s* spectra of $CF_3O_2CF_3$ (band 3) and CF_3OF (band 4) possibly terminate at σ^*(C–O) orbitals, while in the O 1*s* spectra the corresponding transitions are band 3 in $CF_3O_2CF_3$ and band 4 in CF_3OF.

Preceding the CF_3 group signature, there is a weak broad band in the C 1*s* spectrum of $CF_3O_2CF_3$ centered at 294.8 eV (band 1) having a term value of 6.0 eV. On the basis of its large term value, this transition would appear to be C $1s \rightarrow \sigma^*$(O–O). A similar weak feature with a term value of 7.0 eV is observed in CF_3OF (Fig. 6), and is assigned as a low-lying C $1s \rightarrow \sigma^*$(O–F) promotion. It is noteworthy that the term values of these features are considerably smaller than those of the stronger X $1s \rightarrow \sigma^*$(X–Y) and Y $1s \rightarrow \sigma^*$(X–Y) transitions. A corresponding situation is found in the substituted carbonyls, where transitions from the inner-shell orbitals of the substituent (N 1*s*, O 1*s*, and F 1*s*) to the π^*(C=O) orbital have term values several eV smaller than those originating at the C 1*s* or O 1*s* orbitals of the C=O group.[45] This can be interpreted in terms of an "energy penalty" which must be paid whenever there is an appreciable charge transfer involved, as must occur in transitions from a localized inner-shell orbital to a spatially remote, localized virtual σ^* or π^* valence orbital.

Interpretation of the inner-shell spectra of $(CH_3)_3CO_2C(CH_3)_3$, Fig. 8, follows that given above for $CF_3O_2CF_3$. The excitation from O 1*s* to σ^*(O–O) in this peroxide is observed as an intense transition (band 1) centered at 533.0 eV. Calculation of the term value for this band is hampered by the lack of an experimental O 1*s* ionization potential, however, a reasonable estimate can be made from the ionization potentials of related compounds. From the O 1*s* ionization potentials of HO_2H, $CF_3O_2CF_3$, and $CF_3O_3CF_3$ of 541.8, 541.9, and 541.5/542.7 eV,[41] respectively, we estimate that for $(CH_3)_3CO_2C(CH_3)_3$ to be 541.5 eV. This results in an [O 1*s*, σ^*(O–O)] term value of 8.5 eV for the band at 533.0 eV, to be compared with 8.3 eV for the corresponding band in $CF_3O_2CF_3$.

In the C 1*s* region of $(CH_3)_3CO_2C(CH_3)_3$, Fig. 8, there is again a weak band (285.1 eV) with a term value (7.4 eV with respect to the estimated C 1*s* (C–O) ionization potential) which is just too large for a Rydberg assignment in a molecule of this large size and composition; the upperstate configuration must be (C 1*s*, σ^*) if the transition is due to $(CH_3)_3CO_2C(CH_3)_3$. There then follows a strong band (band 2) with a term value of 2.6 eV relative to the

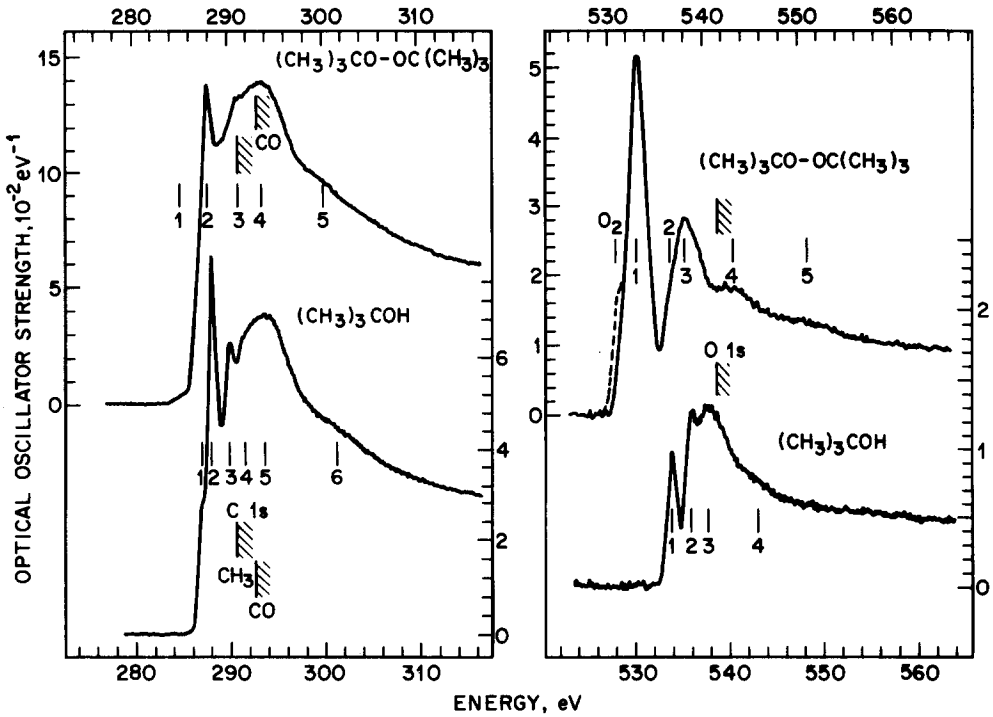

FIG. 8. Optical oscillator strengths derived from the inner-shell energy loss spectra of di(*t*-butyl) peroxide (upper) and *t*-butanol (lower) taken in the region of the C 1*s* (left) and O 1*s* ionization potentials (right). The final electron energy is 2.5 keV, the scattering angle is 2°, and the resolution is 0.6 eV FWHM. The signal due to a small amount of O_2 [dashed line in the O 1*s* spectrum of di(*t*-butyl) peroxide] has been subtracted from the raw data to produce the full curve shown here. The spectra are aligned at the ionization potentials. Thus the energy scales are identical in the C 1*s* spectra whereas the O 1*s* spectra are offset by 3.1 eV with respect to one another. The upper scale is appropriate to $(CH_3)_3CO_2C(CH_3)_3$ and the lower scale to $(CH_3)_3COH$.

C 1*s*(CH_3) ionization potential which is attributed to unresolved excitation from C 1*s* to 3*s*/σ^* and 3*p*/σ^*. Because the *t*-butyl group is close to the alkyl limit, the difference of term values involving 3*s* and 3*p* orbitals is close to zero.[1] On the other hand, the corresponding transitions are somewhat resolved in $CF_3O_2CF_3$ because the molecule is close to the perfluoro limit, where 3*s* and 3*p* term values are separated by up to 3 eV. Bands similar to that observed in $(CH_3)_3CO_2C(CH_3)_3$ at 288 eV are observed in the C 1*s* spectra of neopentane and other saturated alkanes, where the σ^*(C–H) character of the upper obital has been emphasized by a 3*p*/σ^*(CH_3) labeling.[29] The C 1*s* spectrum of $(CH_3)_3CO_2C(CH_3)_3$ is dominated by the C 1*s*→σ^*(C–C) shape resonance (band 4) appearing at 293.5 eV. There is no

TABLE VI. Inner-shell excitations (ΔE, eV), term values (TV, eV), and oscillator strengths (f, 10^{-2}) in CF_3OOOCF_3.

C 1*s*				O 1*s*				F 1*s*				
Band	ΔE	TV	f	Band	ΔE	TV	f	Band	ΔE	TV	f	Assignment
1	294.8	6.0	4.2	1	533.6[a]	8.3	12.0					σ^*(O–O)
2	297.2	3.6						1	690.3	4.4		3*s*/σ^*
3	297.7[b]	3.1	75	2	540.4	1.5	12	2	693.2[c]	1.5	48	3*p*/σ^*(C–F)
4	298.8	2.0										3*p*′
5	299.8	1.0		3	542.4	−0.5		3	695	−0.3		σ^*(C–O)
	300.78[d]				541.93[d]				694.74[d]			IP
6	313	−12		4	555	−13		4	711	−16		EXAFS?

[a] Calibrated as 132.6 eV above the N 1*s*→π^* transition of N_2.
[b] Calibrated as 10.30 eV above the C 1*s*→π^* transition of CO.
[c] Calibrated as 159.6 eV above the O 1*s*→σ^*(O–O) transition of $CF_3O_2CF_3$.
[d] Reference 44.

TABLE VII. Inner-shell excitations (ΔE, eV), term values (TV, eV), and oscillator strengths (f, 10^{-2}) in $(CH_3)_3CO_2C(CH_3)_3$ and $(CH_3)_3COH$.

C 1s										
$[(CH_3)_3CO]_2$					$(CH_3)_3COH$				Assignment	
Band	ΔE	TV(CH_3)	TV(CO)	f	Band	ΔE	TV(CH_3)	TV(CO)	f	CH_3	CO
1	285.1		7.4	0.6							σ^*(O–O)
					1	287.0	3.5		12	$3s/\sigma^*$	
2	287.9[a]	2.6		28	2	287.9[b]	2.6			$3p/\sigma^*$(C–H)	
					3	289.8	0.7	2.7	7.9		$3p/\sigma^*$(C–H)
	290.5[c]					290.5[c]				IP	
3	291.3		1.2		4	291.5		1.0			σ^*(C–O)
	292.5[d]					292.5[d]					IP
4	293.5	−3.0			5	293.6		−3.1		σ^*(C–C)	
5	300	−9			6	301	−10			σ^*(C–C)	

O 1s							
$[(CH_3)_3CO]_2$				$(CH_3)_3COH$			
Band	ΔE	TV	f	Band	ΔE	TV	f	Assignment
1	533.0[e]	8.5	13.9					σ^*(O–O)
2	536.5	5.0						3s
				1	533.9[f]	4.5	1.4	$3s/\sigma^*$(O–H)
				2	535.9	2.5	1.8	3p
3	538.2	3.3		3	537.7	0.7		σ^*(C–O)
	541.5[g]				538.4[h]			IP
4	543	−1.5						σ^*(C–C)?;2e?
5	551	−9		4	543	−4.6		EXAFS?

[a] Calibrated as 2.80 eV below the C $1s\rightarrow\pi^*$ transition of CO_2 (290.74 eV).
[b] Calibrated as 2.83 eV below the C $1s\rightarrow\pi^*$ transition of CO_2 (290.74 eV).
[c] Estimated from the ionization potentials of neopentane (290.4 eV) and *t*-butanol (290.5 eV) (Ref. 41).
[d] Estimated from the ionization potentials of CH_3OH (292.4 eV) and the methylene carbon of C_2H_5OH (292.5 eV) (Ref. 41).
[e] Calibrated as 245.24 eV above feature 1 in $(CH_3)_3CO_2C(CH_3)_3$.
[f] Calibrated as 3.06 eV above the O $1s\rightarrow\pi^*$ transition of O_2 (530.8 eV).
[g] Estimated from the ionization potentials of HOOH (541.8 eV), CF_3OOCF_3 (541.93 eV), and $CF_3O_3CF_3$ (541.5 eV for the external oxygens) (Ref. 41).
[h] From Ref. 41.

corresponding feature in the spectrum of $CF_3O_2CF_3$, as expected. Because the transition to σ^*(C–C) is weak in the O 1*s* spectrum and that to σ^*(O–O) is weak in the C 1*s* spectrum, it is clear that there is very little mixing of the σ^*(C–C) and σ^*(O–O) bond orbitals in $(CH_3)_3CO_2C(CH_3)_3$.

In order to validate the assignment of the 533.0 eV band of $(CH_3)_3CO_2C(CH_3)_3$ as O $1s\rightarrow\sigma^*$(O–O), we recorded the spectra of $(CH_3)_3COH$. These alcohol spectra should differ from those of the peroxide in two respects: (1) the alcohol will not show a transition to σ^*(O–O) in the O 1*s* spectrum, and (2) transitions common to the alcohol and peroxide will have only half the intensity in the former as compared to the latter. The inner-shell spectra of di(*t*-butyl) peroxide and *t*-butanol are compared in Fig. 8, with energy scales chosen so as to align the relevant ionization potentials. As expected, the alcohol spectrum shows no band corresponding to that in the peroxide at 533.0 eV, and though the C 1*s* and O 1*s* spectra are otherwise closely similar, those for the alcohol are only ~50% as intense as those for the peroxide (see also Table IV). Thus comparison of the peroxide and alcohol spectra nicely confirms our assignment of the low-lying O 1*s* and C 1*s* bands in the former as terminating at σ^*(O–O).

Other differences exist between the O 1*s* spectra of *t*-butanol and di(*t*-butyl) peroxide. The band at 533.9 eV (TV = 4.5 eV) in the alcohol does not have a clear counterpart in the peroxide. A well-resolved, low-lying band of similar intensity is observed in the O 1*s* spectra of methanol[31] and the higher alcohols,[48] suggesting that this is a transition terminating at an orbital of mixed $3s/\sigma^*$(O–H) composition characteristic of the –OH group. Another difference is the energies of the features we have attributed to O 1*s* $\rightarrow\sigma^*$(C–O) promotions on the basis of the bond-length correlation.[21] This difference is discussed further in Sec. III E.

C. Weak-bond effects in the spectra of other compounds

1. Halides

In regard weak-bond molecules, the alkyl halides are especially interesting, for they offer many examples of undisputed excitations to low-lying σ^* MOs. Furthermore, because the series CH_3X (X = F, Cl, Br, I) is one of constant geometry but variable C–X bond strength, it allows a more straightforward view of the relation between transition energy and bond strength. As previously discussed for the methyl halides,[1,4] the term values of the $np\pi\rightarrow\sigma^*$(C–X) $\mathscr{A}$ bands in the UV spectra ($np\pi$ is the $p\pi$ lone-pair orbital of principal quantum number n on the halogen atom) and the C $1s\rightarrow\sigma^*$(C–X) bands of the x-ray spectra increase linearly

with decreasing C–X bond strength. Thus, for CH_3I with a C–I bond strength of only 55 kcal/mol (region I), the (C 1*s*, σ^*) term value is 5.65 eV, which places it far below the C 1*s*→3*s* Rydberg transition. On the other hand, in CH_3F the relevant bond strength is increased to 110 kcal/mol (region II), and the lowest excitation to σ^*(C–F) is extrapolated to be almost degenerate with the transition to 3*s* (4.52 eV term value). The excitations to σ^* in CH_3Br and CH_3Cl are intermediate with respect to the extreme situations offered by CH_3I and CH_3F.[12] Alkylation of a methyl halide depresses the ($np\pi$, σ^*) term value in the ultraviolet spectra, and the (C 1*s*, σ^*) term value will likely decrease as well. In accord with the decreasing C–X bond strength, the term values of transitions to σ^*(C–X) increase on going from CH_3X to CX_4.[49]

The situation in the boron halides parallels that in the alkyl halides. Thus in BCl_3 and BBr_3,[25] the B 1*s*→σ^* transitions have positive term values of 2.85 and 3.22 eV, respectively; the B–X bond strength in BCl_3 is 110 kcal/mol. On the other hand, in BF_3 one has a B–F bond strength of 153 kcal/mol (region III) and a negative (B 1*s*, σ^*) term value of -2.29 eV.[25] It is in this paper on the boron halides[25] that one finds the first mention in the literature to our knowledge of the influence of bond strength on the energy of excitations to a σ^* MO.

Spectral data is available in the literature on two saturated molecular fluorides having very weak bonds. One is KrF_2, with an average Kr–F bond strength of only 10.6 kcal/mol. In the Kr 1*s* spectrum of this molecule there is an intense transition at 14 319 eV, approximately 10 eV below the Kr 1*s* ionization potential.[50] The upper state clearly involves the σ^*(Kr–F) MO as terminating orbital. This σ^* MO of KrF_2 is closely related to that involved in the 4*d*→σ^* transition in the weak-bond molecule XeF_6, where the (4*d*, σ^*) term value is 10 eV.[1]

In the F 1*s* spectrum of F_2, the excitation to σ^*(F–F) leads the parade, with a term value of 14.5 eV![51] As might be expected for such a large term value, the F–F bond strength is rather small, being only 36 kcal/mol, Table III. Thus it is seen that as one goes from BF_3 to F_2 in the first-row fluorides, the inner-shell excitations to σ^*(X–F) move smoothly from region III to region I behavior, paralleling the X–F bond strengths.

In the context of the orbital ordering in F_2, the situation in regard the position of the σ^* MO in HF is most interesting. Inasmuch as the H–F bond strength is 134 kcal/mol,[14] we expect the [F 1*s*, σ^*(H–F)] term value to be considerably smaller than the 14.5 eV observed for F_2. Indeed, according to Hitchcock and Brion,[51] the first excitation in HF originating at F 1*s* has a term value of 6.7 eV (5.8 eV in the outer shell spectrum[52])], and in each case corresponds to an excitation terminating at σ^*(H–F) rather than at 3*s*. The assignment of these bands as valence excitations at first sight seems unlikely considering that the H–F bond strength places it solidly in region III, which implies a negative term value. Similarly, low-lying excitations to σ^* (H–X) are found in the Br 3*d* spectrum of HBr[53] and the I 4*d* spectrum of HI,[54] and yet the bond energies of 86 and 70 kcal/mol, respectively, would suggest that these molecules are more likely region II species in which strong valence–Rydberg mixing is to be expected. The lesson to be learned here is that whereas weak bonds imply low-lying σ^* MOs, the reverse is not necessarily true. Thus in C_6F_6[55] and in $F_2C{=}CF_2$[1,27] one again encounters low-lying σ^* MOs, but the cause lies with the differential depression of σ and σ^* MOs by fluorination in planar systems (the perfluoro effect[35,47,56]) rather than with weak bonds.

2. Other systems

It was seen above that going from H_2O to F_2O introduced a weak bond into the molecule, the spectral response being the appearance of intense, low-lying transitions to the σ^*(O–F) MO in both the inner-shell and outer-shell spectra. Similarly, introduction of the weak bond on going from H_2O to HO–OH again should introduce low-lying transitions to σ^*(O–O) in the peroxide's inner-shell and outer-shell spectra. Indeed, unlike the situation in H_2O, in HO–OH the Rydberg manifold in the outer-shell spectrum is preceded by two valence excitations to σ^*(O–O).[57] Closely similar inner shell and outer shell excitations to σ^*(O–O) are expected at low energies in higher alkyl peroxides, oxetanes, and peracids.

It has been noted[1] that the UV spectra of the methylated polysilanes $H_3C[Si(CH_3)_2]_nCH_3$ are very different from those of the corresponding alkanes, the reason being that the polysilanes have relatively weak Si–Si bonds (51 kcal/mol in H_3Si–SiH_3) compared to the C–C bonds of the alkanes (80 kcal/mol in H_3C–CH_3). As a consequence, the polysilanes are in region I (Fig. 1) and in fact do show low-lying $\sigma\rightarrow\sigma^*$ excitations,[58] whereas the corresponding ultraviolet excitations in alkanes have yet to be found. On this basis, we similarly expect the x-ray spectra of the polysilanes to exhibit low-lying excitations from Si 2*p* to σ^*(Si–Si) MOs, and indeed, recent photoionization studies[59] reveal that $Si_2(CH_3)_6$ exhibits a feature at 102.2 eV having a 4 eV term value which is assignable as Si 2*p*→σ^*(Si–Si) since it is 2 eV below the lowest energy feature in the Si 2*p* spectrum of $Si(CH_3)_4$.[60] The characterization of the Si 2*p* spectrum of $Si_2(CH_3)_6$ by photoionization mass spectometry[59] offers the possibility of testing the Si 2*p*→σ^*(Si–Si) assignment, for one expects a fragmentation pattern exhibiting enhanced Si–Si bond breaking in the [Si 2*p*, σ^*(Si–Si)] excited state.

A number of other molecular systems are good candidates for low-lying σ^* MOs on the basis of their region I bond energies. Beside those in Table I, we list CF_3O–O–OCF_3, (NO_2)–(NO_2), RO–NO, RO–NO_2, $C_6H_5CH_2$–$CH_2C_6H_5$, and C_2H_5–Hg–C_2H_5 as compounds which should be studied. As our inner-shell spectrum[61] of N_2H_4 (N–N bond energy of 60 kcal/mol) did not show a low-lying excitation to σ^*(N–N), this sytem apparently is in region II; however, N_2F_4, with an N–N bond energy of only 21 kcal/mol (Table I) is certain to exhibit region I spectral behavior. In light of our concern with bond strengths and their effect on inner-shell spectra, the addition compound formed between BF_3 and H_2O is most intriguing. In this complex, the component molecules have quite strong bonds whereas the complex itself is joined by a B–O bond having an

energy of only ~16 kcal/mol.[18] Consequently, we expect transitions to σ^*(B–O) in the complex which lie far below any of those in the component molecules. Indeed, in the outer-shell spectrum of the complex, there are *four* excitations reported in the 1–5 eV region whereas the lowest band of H_2O is at 7.4 eV and that of BF_3 is at 7.9 eV.[18] Thus we expect that the B 1*s* and O 1*s* spectra of the complex will show transitions to σ^*(B–O) of extraordinarily large term values, and that these transitions will be missing from the F 1*s* spectrum for reasons of overlap. The $BF_3 \cdot H_2O$ complex is but an example of an entire class of complexes involving Lewis acids and bases. To the extent that the donors and acceptors in these complexes are bound by 10–30 kcal/mol, each is an excellent prospect for a low-lying transition to σ^*.

The spectroscopic consequences of a weak bond extend beyond inner-shell and valence-shell excitation. Recent work has shown that the energies of $1s \rightarrow \sigma^*$ valence excitations correlate with those temporary-negative-ion (TNI) resonances of the molecule in which the incident electron is captured in a σ^* MO.[47,55,62] Expanding upon this idea, the relatively low energies of the $1s \rightarrow \sigma^*$ bands in weak-bond molecules suggests that σ^* TNI resonances in these molecules also will occur at relatively low energies. This is evident in the chloromethanes,[63] where negative ion resonances appear several eV below the lowest in methane. Similarly, those cyclic perfluoroalkanes which exhibit a low-lying inner-shell excitation to σ^* also show negative-ion resonances at much lower energies than those of the acyclic systems.[46]

Let us extend our thinking one step beyond weak σ bonds. Though the σ^*(C–C) bond in ethylene is a strong one, the barrier to rotation due to the π MOs is only 50–60 kcal/mol. Thus one can think of the π component of the C–C bonding in ethylene as consisting of a weak two-electron/two-center bond (region I) capable of resulting in a C $1s \rightarrow \pi^*$ transition in ethylene which lies below the $1s \rightarrow 3s$ Rydberg band, but probably not by much. This, of course, is just the case, the (C 1*s*, π^*) term value in ethylene being 5.4 eV, whereas the (C 1*s*, 3*s*) term value is only 2.6 eV.[27,47] Similarly, in the outer-shell spectrum of ethylene, $\pi \rightarrow 3s$ precedes $\pi \rightarrow \pi^*$ by 0.5 eV in the singlet manifold. When viewed in this way, one sees that the spectra of olefins are not that different from those of saturated molecules, as they closely resemble those in region I having weak bonds.

D. Oscillator strengths

The Bethe–Born theory of charged-particle scattering[64] provides a well-defined relationship between inelastic electron scattering cross sections and optical oscillator strengths in the regime of small momentum transfer (q), i.e., small angle scattering, and at energy losses small with respect to the impact energy. According to this treatment, the shapes of the optical and energy loss spectra are related by a factor of E^{-3}, in the limit of zero momentum transfer. Since q is finite (chiefly because of the energy transfer term Θ_E) and has a range of values due both to the finite divergence of the electron beam and the angular acceptance of the electron analyzer (Θ_M), the effective relationship between the two types of spectra is somewhat different from the idealized E^{-3} proportionality. Our approach is outlined below.

After a background subtraction obtained from extrapolation of a least-squares fit of the pre-edge data to $c(E-b)^a$ with a approximately 4, the relative optical cross section $\sigma_{\text{opt}}^{\text{rel}}$ was obtained from the relative energy loss cross section $\sigma_{\text{el}}^{\text{rel}}$ using the formula of Leapman *et al.*[65]:

$$\sigma_{\text{opt}}^{\text{rel}} = \sigma_{\text{el}}^{\text{rel}} / \log\left\{1 + \left(\frac{\Theta_M}{\Theta_E}\right)^2\right\},$$

where $\Theta_E = E/2(E + 2500)$ for our spectrometer operating with a constant final electron energy of 2.5 keV, and Θ_M was taken as 2°. Over a typical 50 eV range, this shape correction factor tilts the energy loss spectra upward by 32%, 19%, and 15% in the C 1*s*, O 1*s*, and F 1*s* regions. We note that other correction formulas exist[66] which differ slightly from that given above.

The relative optical spectra were then converted to absolute intensities using a one-point normalization to the calculated atomic oscillator strength for the relevant inner-shell photoionization[67] at an energy 25 eV above the ionization potential. Thus, for example, for $CF_3O_2CF_3$ the normalization factors in units of 10^{-2} eV^{-1} were 2×0.77, 2×0.45, and 6×0.37 for the C 1*s*, O 1*s*, and F 1*s* relative optical spectra. This approach assumes that molecular effects are negligible 25 eV above an ionization edge and that the atomic calculations are accurate. A more complete discussion of this normalization technique, its systematic errors and demonstration of its ability to reproduce direct measurements of inner-shell optical oscillator strengths is presented elsewhere.[27] When tested against independent measurements, our absolute intensities are found to be uncertain to $\pm$ 20%.

The oscillator strengths determined from integrated areas of resolved peaks or groups of peaks are summarized in the spectral data Tables (II, V, VI, and VII). In addition, the total integrated intensities in the discrete and near-continuum (threshold to 25 eV above the ionization potential) are presented in Table IV, and the sums of X $1s \rightarrow \sigma^*$(X–Y) and Y $1s \rightarrow \sigma^*$(X–Y) oscillator strengths for all σ^*(X–Y) in this series of compounds appear in Table VIII. It is noteworthy that the features terminating at σ^*(X–Y) in an XYZ molecule are observed to be more intense in the X 1*s* or Y 1*s* spectra than in the Z 1*s* spectra [part (viii) of Sec. III A], although weak Z $1s \rightarrow \sigma^*$(X–Y) features can be identified [e.g., O $1s \rightarrow \sigma^*$(C–F) transitions in CF_3OF and CF_3OOCF_3]. It is also interesting that there seems to be a roughly constant intensity *per* σ^* *transition* for each type of σ^* (see Table VIII). The intensities of $1s \rightarrow \sigma^*$ transitions increase as Z and the term values increase (i.e., as the σ^* orbital becomes more bound and more localized). There also is a trend to smaller $1s \rightarrow \sigma^*$(C–O) intensity as the number of electronegative atoms in the molecule, and thus the potential barrier, decreases. This parallels the effect of changes in the strength of the potential barrier on the intensities of C 1*s* and F $1s \rightarrow \sigma^*$(C–F) transitions that has been documented in the series C_6F_6, C_2F_4, C_2F_6, and CF_4.[68]

The effects of potential barriers on the inner-shell spec-

TABLE VIII. Systematics of $1s\rightarrow\sigma^*$ oscillator strengths.

Bond	Z	TV_{avg}	$\Sigma f/n$[a] FOF	CF_3OF	$CF_3O_2CF_3$	$[(CH_3)_3CO]_2$	$(CH_3)_3COH$
O–F	17	11.0	9.7	11.9			
O–O	16	8.4			12.0	13.9	
C–F	15	2.2		(5.8)	(5.0)		
C–O	14	0.9		(4.2)	(3.9)	(1.9)	(2.1)
C–C	12	−3.1				(0.5)	(0.5)

[a] Summed oscillator strengths (10^{-2}) of $1s\rightarrow\sigma^*$(X–Y) in the X 1*s* and Y 1*s* spectra, divided by the number of X–Y bonds in the molecule. The values in parentheses are peak (10^{-2} eV^{-1}) rather than integrated intensities.

tra of our weak-bond compounds also are evident in the increased intensity below the ionization thresholds in the more highly fluorinated molecules (Table IV). This arises primarily because of the enhanced oscillator strengths to spatially localized inner-well orbitals which are low lying and have large overlaps with the originating orbital. In addition, the intensities of the near-continuum regions of the more highly fluorinated compounds decrease on a per-atom basis, presumably because the potential barrier excludes inner-shell ion states with low photoelectron kinetic energies.[37] Both effects contribute to the dramatic changes of the discrete /continuum intensity ratios observed for the C 1*s* and O 1*s* spectra (Table IV).

The regularities of the oscillator strengths for corresponding $1s\rightarrow\sigma^*$(X–Y) transitions in different molecules are remarkable. Because the σ^*–σ^* splitting between the two local σ^*(O–F) bonds of F_2O is only 1–2 eV, one expects that in CF_3OF with only a single O–F bond, the [1*s*, σ^*(O–F)] term values in this molecule will lie close to those of F_2O. As seen in Table II, this is the case. Arguing further along the line of weakly interacting σ^*(O–F) group orbitals, one expects that the oscillator strength of the F $1s\rightarrow\sigma^*$(O–F) transition in F_2O will be twice that of the same transition in CF_3OF. Similarly, the oscillator strength ratio of the corresponding transitions originating at O 1*s* should equal 2. Experimentally, the ratio of the F $1s\rightarrow\sigma^*$(O–F) oscillator strengths in F_2O and CF_3OF is 1.69, while the ratio of O $1s\rightarrow\sigma^*$(O–F) oscillator strengths in the same compounds is 1.58.

Turning to the peroxides, the O $1s\rightarrow\sigma^*$(O–O) transitions might be expected to have equal oscillator strengths in $CF_3O_2CF_3$ and $(CH_3)_3CO_2C(CH_3)_3$; the measured ratio is 0.86. Somewhat more surprising is the comparison of intensities between O–O and O–F chromophores. In the simplest picture one expects the sum of the O $1s\rightarrow\sigma^*$(O–F) and F $1s\rightarrow\sigma^*$(O–F) oscillator strengths in CF_3OF to roughly equal that of the O $1s\rightarrow\sigma^*$(O–O) transition in $CF_3O_2CF_3$. In fact, a ratio of 0.98 is observed.

That the excitations to σ^*(O–O) in the peroxides and to σ^*(O–F) in CF_3OF and F_2O have intensities predominantly in the appropriate O 1*s* and F 1*s* spectra, and the fact that their oscillator strengths scale rather well with the numbers of O and F atoms in the weak bonds both suggest that the O–O and O–F bonds are highly localized in these compounds. Inasmuch as these weak-bond group orbitals are very localized and have little or no Rydberg character in the antibonding levels, it is understandable why there appears to be a sum rule on the oscillator strengths of transitions to them from 1*s*. However, one factor must be recognized in this: the $1s\rightarrow 2p$ atomic transition moment for the O atom is about 20% larger than for the F atom.

E. Bond lengths from $1s\rightarrow\sigma^*$ term values

According to Refs. 15 and 21 there is a simple, linear relationship between the term values of $1s\rightarrow\sigma^*$(X–Y) transitions and the X–Y bond lengths, within classes of molecules of similar potentials in the region of the X–Y bond. For convenience these classes have been identified by a parameter Z, the sum of the atomic numbers of X and Y. This very localized picture was derived from the spectra of diatomics and "pseudodiatomics." The applicability of this picture to polyatomics containing different types of X–Y bonds (a theme of several recent studies[28,29,45,69]) would seem to depend in large part on the degree of localization of the σ^* molecular orbitals. Thus, in this work, it is not surprising that good agreement with the correlation[15,21] is found for transitions to the obviously very localized σ^*(O–F) orbitals in F_2O and CF_3OF and the σ^*(O–O) orbitals in the peroxides. Possibly more surprising is the level of agreement that is found between the molecular structure and the positions of features attributed to $1s\rightarrow\sigma^*$(C–O), σ^*(C–F), and σ^*(C–C) transitions in these molecules. The bond length-term value correlations for all five molecules of this study are summarized in Table IX. The features associated with transitions to σ^* (C–O), σ^*(C–F), and σ^*(C–C) provide correlation-predicted bond lengths that are in good agreement with literature values,[22,27] or with estimated bond lengths where experimental values are not available. One interesting point is the increased term value of the feature attributed to the $1s\rightarrow\sigma^*$(C–O) transition on going from $(CH_3)_3COH$ to $(CH_3)_3COOC(CH_3)_3$. This shift (which is particularly clear in the O 1*s* spectra) can be interpreted in terms of bond lengthening of 0.03 to 0.06 Å (depending on whether one uses the average of the C 1*s* and O 1*s* or just the O 1*s* term value). Alternatively, the shift may not be solely geometric in origin but rather partially connected with an energy split-

TABLE IX. Correlation of X $1s\rightarrow\sigma^*$(A–B) term values (TV, eV) and bond lengths (R, Å).

Molecule	X	A–B	Z	Band	TV[a]	TV_{av}[b]	R_{calc}[c]	R_{obs}[d]
F_2O	O	O–F	17	1,2	10.1[e]	10.6	1.33	1.405
	F	O–F	17	1,2	11.1[e]			
CF_3OF	O	O–F	17	1	11.1	11.0	1.35	1.421
	F	O–F	17	1	11.0			
	C	C–F	15	3	3.1	2.1	1.32	1.319
	F	C–F	15	3	1.3			
	[O	C–F	15	3	2.8][f]			
	C	C–O	14	5	1.1	0.8	1.44[g]	1.395
	O	C–O	14	4	0.5			
CF_3OOCF_3	O	O–O	16	1	8.3	8.3	1.42	1.419
	[C	O–O	16	1	6.0]			
	C	C–F	15	3	3.1	2.3	1.33	1.320
	F	C–F	15	2	1.5			
	[O	C–F	15	2	1.5]			
	C	C–O	14	5	1.0	0.3	1.43[g]	1.399
	O	C–O	14	3	−0.5			
$[(CH_3)_3CO]_2$	O	O–O	16	1	8.5	8.5	1.43	(1.44)
	[C	O–O	16	1	7.4]			
	C	C–O	14	2	1.2	2.1	1.46[g]	(1.45)
	O	C–O	14	3	3.3			
	C	C–C	12	4	−3.0	−3.0	1.50	(1.53)
	[O	C–C	12	4	−1.5]			
$(CH_3)_3COH$	C	C–O	14	4	1.0	0.8	1.44[g]	(1.43)
	O	C–O	14	3	0.7			
	C	C–C	12	5	−3.1	−3.1	1.50	(1.53)
	[O	C–C	12	4	−4.6]			

[a] See Tables II–V for the transition energies and ionization potentials used to obtain term values.

[b] For X–Y bonds where $1s\rightarrow\sigma^*$(X–Y) transitions are observed in both the X 1s and the Y 1s spectra, the average of the two term values is used in the correlation. Note that where there is a large difference in the atomic number of X and Y, the X 1s and Y 1s term values can be several eV different {e.g., TV [C $1s\rightarrow\sigma^*$(C–F)] is ~2 eV greater than TV [F $1s\rightarrow\sigma^*$(C–F)]}.

[c] Predicted from the least-squares correlation lines reported in Ref. 15 except for the values for $Z = 17$, where the distances were obtained from: $T = -14.06 + 18.57R$. This is derived from $Z = 17$ data obtained by extrapolation of a family of least-squares curves as in Fig. 4 for $R = 1.20, 1.25, 1.30, 1.35, 1.40, 1.45$ Å.

[d] Data from electron diffraction (Ref. 16). Values listed in parentheses have been estimated from standard bond lengths (C–C, C–O) or from similar compounds. Note that the O–O bond length in the peroxides is difficult to estimate accurately since R(O–O) = 1.475 Å in HOOH but 1.217 Å in FOOF. The latter is anomalously short because of ionic contributions.

[e] Resolved maxima of the $1s\rightarrow\sigma^*$(O–F) peaks. This corresponds to an intensity-weighted average of the transitions to $a_1\sigma^*$(O–F) and $b_2\sigma^*$(O–F).

[f] Data in brackets are from the 1s spectra of atoms not involved in the indicated bond. Their term values are not used in calculating TV_{av}.

[g] There is a misprint in Table II of Ref. 15. The parameters for $Z = 14$ based on the data of Table I of Ref. 15 for $\delta = m - n^*R$ should be m(eV) = 42.19 and n(eV Å^{-1}) = 29.81.

ting between symmetric and antisymmetric combinations of the two localized σ^*(C–O) orbitals in t-butyl peroxide. The higher lying O $1s\rightarrow\sigma^*$(C–O) transition could then be assigned to feature 4, which is more intense in the O 1s spectrum of the peroxide than in the alcohol.

In addition to the principal $1s\rightarrow\sigma^*$ transitions, there are weaker features in the continua of many of these spectra which in some cases could be additional one-electron excitations to higher-lying σ^* levels. This explanation for the 300 eV features in $(CH_3)_3CO_2C(CH_3)_3$ and $(CH_3)_3COH$ is identical to that suggested for similar features in the C 1s continua of alkanes[29] and cyclic alkanes.[69] However, these continuum features are very weak compared to the principal $1s\rightarrow\sigma^*$(X–Y) transitions and thus they do not generate any ambiguity in the bond length correlation (in contrast to cases like the aromatics,[28] where the $1s\rightarrow\sigma^*$ intensity appears to be split nearly equally among several, widely dispersed transitions). Of course there are other possibilities for these broad, weak continuum features (e.g., double excitation, shake-up continua, or EXAFS). Calculations and complementary spectroscopic studies are desirable to clarify the origin of these features. The continuum peaks in the O 1s and F 1s spectra of F_2O are particularly intriguing since there are no high-lying σ^* molecular orbitals upon which to base one-electron excitations. F_2O could be another example, like CF_4,[70] where there is not a one-to-one correspondence between core excitation shape resonances and minimal basis set, unoccupied MOs.[8] Given the relative simplicity of F_2O it would appear to be a particularly worthwhile target for detailed theoretical study.

IV. OVERVIEW

We see from the present work that certain weak-bond molecules exhibit intense, low-lying $1s\rightarrow\sigma^*$ excitations having characteristic term values: for transitions to σ^*(F–F),

σ^*(O–F), and σ^*(O–O) MOs, the term values are 14.5, 11.3, and 8.5 eV, respectively. On the other hand, the bond energies for the F–F, O–F, and O–O (peroxide) bonds are nearly the same (36–46 kcal/mol, Table I). This shows that while there is qualitative value to the weak-bond concept in spectroscopy, there is no simple quantitative relation between σ^* term values and bond energies. The discrepancy arises because the σ^* term value will depend not only on the σ–σ^* split (a nondiagonal term in the energy, quantity S in Fig. 1) but also on the energies (electronegativities) of the component AOs at infinite separation (a diagonal term in the energy, quantity Q in Fig. 1). This latter factor increases systematically with the atomic number for first-row atoms. It is partly because Q plays as large or a larger role than S in determining ($1s^{-1}$, σ^*) term values that the term-value data for first-row fluorides (Table III) provides a better correlation with Z (TV $= -61.3 - 4.24Z$, with a correlation coefficient of 0.998) than with the bond energy BE (TV $= 16.9 - 0.128$ BE, with a correlation coefficient of 0.973).

Similarly, it is because the $2p$ ionization potential (term value) of F is $\sim$6 eV larger than that of O, that the F–F bond has a σ^* term value $\sim$6 eV larger than that for O–O even though the bond energies are essentially equal. Interestingly, the σ^*(O–F) term value is just equal to the average of the σ^*(F–F) and σ^*(O–O) term values. In light of these trends, the value of the σ^*(N–N) term values in F_2N–NF_2 is of interest. The low nuclear charge of N will act to make the [$1s$, σ^*(N–N)] term value small, however this will be countered by the small σ–σ^* split implied by the N–N bond energy of only 21 kcal/mol. This molecule is now under study.

The idea that a weak X–Y bond implies a low-lying σ^* (X–Y) MO as depicted in Fig. 1 is in harmony with the results of several calculations on the Rydberg/valence nature of upper states as a bond in the molecule is stretched.[1] Taking CH_4 as an example,[71] *ab initio* calculations show that at the equilibrium geometry of the ground state, the lowest excited state is ($t_2\sigma$, $3s$). However, as one C–H bond is lengthened, the Rydberg character of the upper orbital rapidly decreases, so that after an extension of 0.5 Å, the upper orbital has been transformed into the valence MO $a_1\sigma^*$(C–H). This de-Rydbergization can be understood in terms of Fig. 1 in the following way. In its ground-state equilibrium geometry, methane is a region II system in which the σ^* MO is dissolved in the Rydberg sea. However, as the C–H bond is progressively lengthened and weakened, a region I situation develops in which the σ^* MO eventually drops below the Rydberg manifold and so assumes its full valence character. In parallel with this avoided curve crossing which converts the lowest Rydberg MO into a σ^* MO, there also is a σ^* MO at higher energy which is converted by the same process into a Rydberg MO.[71] Similar region II $\rightarrow$ region I de-Rydergization has been calculated to occur in C_2H_5, SiH_4, NH_3, PH_3, CH_3, and H_2O as one M–H bond is lengthened in each.[1]

ACKNOWLEDGMENTS

Financial support in the form of research grants and a University Research Fellowship (A.P.H.) was provided by NSERC (Canada). A.P.H. thanks LURE and the government of France for their hospitality during a sabbatical leave during which this paper was written. We are indebted to Professor W. H. E. Schwarz for comments on this work.

[1] M. B. Robin, *Higher Excited States of Polyatomic Molecules* (Academic, New York, 1974), Vol. I; Vol. II (1975); Vol. III (1985).
[2] R. S. Mulliken, J. Am. Chem. Soc. **86**, 3183 (1964).
[3] M. B. Robin, Chem. Phys. Lett. **119**, 33 (1985).
[4] M. B. Robin, Can. J. Chem. **63**, 2032 (1985).
[5] W. H. E. Schwarz, Chem. Phys. **11**, 217 (1975); **9**, 157 (1975).
[6] H. Freidrich, B. Sonntag, P. Rabe, W. Butscher, and W. H. E. Schwarz, Chem. Phys. Lett. **64**, 360 (1979).
[7] W. H. E. Schwarz, L. Mensching, K. H. Hallmeier, and R. Szargan, Chem. Phys. **82**, 57 (1983).
[8] W. H. E. Schwarz, U. Seeger, and R. Seeger, Chem. Phys. (in press).
[9] H. Lefebvre-Brion, *Proceedings of the International Symposium on Molecules in Physics, Chemistry, and Biology* (Reidel, Dordrecht, to be published). See also, F. Keller and H. Lefebvre-Brion, Z. Phys. D **4**, 15 (1986).
[10] H. Lefebvre-Brion and R. W. Field, *Perturbations in the Spectra of Diatomic Molecules* (Academic, New York, 1986).
[11] R. S. Mulliken, Phys. Rev. **61**, 277 (1942).
[12] A. P. Hitchcock and C. E. Brion, J. Electron Spectrosc. Relat. Phenom. **13**, 193 (1978); **17**, 139 (1979).
[13] A. P. Hitchcock and C. E. Brion, J. Phys. B **14**, 4399 (1981).
[14] T. L. Cottrell, *The Strengths of Chemical Bonds* (Butterworths, London, 1958).
[15] F. Sette, J. Stöhr, and A. P. Hitchcock, J. Chem. Phys. **80**, 4906 (1984).
[16] Landolt-Bornstein, *Structure Data of Free Polyatomic Molecules*, New Series II (Springer, Boston, 1976), Vol. 7.
[17] J. Berkowitz and J. H. Holloway, J. Chem. Soc. Faraday Trans. 2 **74**, 2077 (1978).
[18] M. C. Durrant, M. S. Hegde, and C. N. R. Rao, J. Chem. Phys. **85**, 6356 (1986).
[19] D. F. McMillen and D. M. Golden, Annu. Rev. Phys. Chem. **233**, 493 (1982).
[20] H. J. Svec and G. A. Junk, J. Am. Chem. Soc. **89**, 2836 (1967).
[21] A. P. Hitchcock, S. Beaulieu, T. Steel, J. Stöhr, and F. Sette, J. Chem. Phys. **80**, 3927 (1984).
[22] C. J. Marsden, L. S. Bartell, and F. P. Diodati, J. Mol. Struct. **39**, 253 (1977).
[23] J. Czarnowski and H. J. Schumacher, Z. Phys. Chem. **86**, 7 (1973).
[24] C. J. Czarnowski, E. Castellano, and H. J. Schumacher, Chem. Commun. **1968**, 1255.
[25] E. Ishiguro, S. Iwata, Y. Suzuki, A. Mikuni, and T. Sasaki, J. Phys. B **15**, 1841 (1982).
[26] C. E. Brion, S. Daviel, R. N. S. Sodhi, and A. P. Hitchcock, AIP Conf. Proc. **94**, 426 (1982); A. P. Hitchcock, J. Electron Spectrosc. Relat. Phenom. **25**, 245 (1982).
[27] R. McLaren, S. A. C. Clark, I. Ishii, and A. P. Hitchcock, Phys. Rev. A **36**, 1683 (1987).
[28] J. A. Horsley, J. Stöhr, A. P. Hitchcock, D. C. Newbury, A. L. Johnson, and F. Sette, J. Chem. Phys. **83**, 6099 (1985).
[29] A. P. Hitchcock and I. Ishii, J. Electron Spectrosc. Relat. Phenom. **42**, 11 (1987).
[30] D. A. Shaw, G. C. King, and F. H. Read, Chem. Phys. Lett. **129**, 17 (1986); D. A. Shaw, G. C. King, D. Cvejanovic, and F. H. Read, J. Phys. B **17**, 2091 (1984); L. Ungier and T. D. Thomas, Chem. Phys. Lett. **96**, 247 (1983); D. A. Shaw, G. C. King, F. H. Read, and D. Cvejanovic, J. Phys. B **15**, 1785 (1982); W. H. E. Schwarz and R. J. Buenker, Chem. Phys. **13**, 153 (1976).
[31] G. R. Wight and C. E. Brion, J. Electron Spectrosc. Relat. Phenom. **4**, 25 (1974).
[32] J. W. Koepke and W. L. Jolly, J. Electron Spectrosc. Relat. Phenom. **9**, 413 (1976).
[33] D. W. J. Cruickshank and E. J. Avramides, Philos. Trans. R. Soc. London Ser. A **304**, 533 (1982).

[34]K. E. Valenta, K. Vasudevan, and F. Grein, J. Chem Phys. **72**, 2148 (1980).
[35]C. R. Brundle, M. B. Robin, N. A. Kuebler, and H. Basch, J. Am. Chem. Soc. **94**, 1451 (1972).
[36]W. Von Niessen, J. Electron Spectros. Relat. Phenom. **17**, 197 (1979).
[37]J. L. Dehmer, J. Chem. Phys. **56**, 4496 (1972).
[38]J. Berkowitz, P. M. Dehmer, and W. A. Chupka, J. Chem. Phys. **59**, 925 (1973).
[39]J. F. Olsen, J. Fluorine Chem. **9**, 471 (1977).
[40]M. B. Robin and N. A. Kuebler, J. Electron Spectrosc. Relat. Phenom. **1**, 13 (1972/73).
[41]W. L. Jolly, K. D. Bomben, and C. J. Eyermann, At. Data Nucl. Data Tables **31**, 433 (1984).
[42]R. S. Brown, Can. J. Chem. **53**, 3439 (1975).
[43]C. Glidewell, J. Mol. Struct. **67**, 35 (1980).
[44]P. Brant, J. A. Hashmall, F. L. Carter, R. De Marco, and W. B. Fox, J. Am. Chem. Soc. **103**, 329 (1981).
[45]I. Ishii and A. P. Hitchcock, J. Chem. Phys. **87**, 830 (1987).
[46]I. Ishii, R. McLaren, A. P. Hitchcock, K. D. Jordan, Y. Choi, and M. B. Robin (to be published).
[47]M. B. Robin, R. McLaren, I. Ishii, and A. P. Hitchcock (to be published).
[48]I. Ishii and A. P. Hitchcock, J. Electron Spectrosc. Relat. Phenom. (in press).
[49]A. P. Hitchcock and C. E. Brion, J. Electron Spectrosc. Relat. Phenom. **14**, 417 (1978); F. C. Brown, R. Z. Bachrach, and A. Bianconi, Chem. Phys. Lett. **54**, 425 (1978).
[50]F. W. Kutzler, D. E. Ellis, T. I. Morrison, G. K. Shenoy, P. J. Viccaro, P. A. Montano, E. H. Appelman, L. Stein, M. J. Pellin, and D. M. Gruen, Solid State Commun. **46**, 803 (1983).
[51] A. P. Hitchcock and C. E. Brion, J. Phys. B **14**, 4399 (1981).
[52]A. P. Hitchcock, C. E. Brion, G. R. J. Williams, and P. W. Langhoff, Chem. Phys. **88**, 65 (1984).
[53]D. A. Shaw, D. Cvejanovic, G. C. King, and F. H. Read, J. Phys. B **17**, 1173 (1984).
[54]P. Morin and I. Nenner, Phys. Scr. (in press).
[55]A. P. Hitchcock, P. Fischer, A. Gedanken, and M. B. Robin, J. Phys. Chem. **91**, 531 (1986).
[56]C. R. Brundle, M. B. Robin, and N. A. Kuebler, J. Am. Chem. Soc. **94**, 1466 (1972).
[57]C. Chevaldonnet, H. Cardy, and A. Dargelos, Chem. Phys. **102**, 55 (1986).
[58]R. D. Miller, D. Hofer, J. Rabolt, and G. N. Fickes, J. Am. Chem. Soc. **107**, 2172 (1985).
[59]G. G. B. de Souza, P. Morin, and I. Nenner (private communication).
[60]R. N. S. Sodhi, S. Daviel, C. E. Brion, and G. G. B. de Souza, J. Electron Spectrosc. **35**, 45 (1985); G. G. B. de Souza, P. Morin, and I. Nenner, J. Chem. Phys. **83**, 492 (1985); P. Morin, G. G. B. de Souza, I. Nenner, and P. Lablanque, Phys. Rev. Lett. **56**, 131 (1986).
[61] I. Ishii, M. B. Robin, and A. P. Hitchcock (unpublished).
[62]M. Tronc, L. Malegat, R. Azria, and Y. L. Coat, J. Phys. B **15**, L253 (1982), and references therein.
[63]P. D. Burrow, A. Modelli, N. S. Chiu, and K. D. Jordan, J. Chem. Phys. **77**, 2699 (1982).
[64]M. Inokuti, Rev. Mod. Phys. **43**, 297 (1971).
[65]R. D. Leapman, L. A. Grunes, P. L. Fejes, and J. Silcox, in *EXAFS Spectroscopy*, edited by B. K. Teo and D. C. Joy (Plenum, New York, 1981).
[66]K. E. Johnson, K. Kim, D. B. Johnson, and S. Lipsky, J. Chem. Phys. **70**, 2189 (1979).
[67]G. Doolan and D. Liberman, Lawrence Livermore Labs, 1986 (unpublished).
[68]A. P. Hitchcock, P. Fischer, and R. McLaren, *Proceedings of NATO ASI Giant Resonances in Atoms, Molecules and Solids*, Les Houches, France (Plenum, New York, 1987), p. 281.
[69]A. P. Hitchcock, D. C. Newbury, I. Ishii, J. Stöhr, J. A. Horsley, R. D. Redwing, A. L. Johnson, and F. Sette, J. Chem. Phys. **85**, 4849 (1986).
[70]J. A. Stephens, D. Dill, and J. L. Dehmer, J. Chem. Phys. **84**, 3638 (1986).
[71]M. S. Gordon, Chem. Phys. Lett. **52**, 161 (1977).